

EXERGY AND ECONOMIC ANALYSES OF POLYMER ELECTROLYTE MEMBRANE (PEM) FUEL CELL SYSTEM CONFIGURATIONS

BY

SANI AYUBA

DEPARTMENT OF CHEMICAL ENGINEERING,
FACULTY OF ENGINEERING
AHMADU BELLO UNIVERSITY, ZARIA
NIGERIA

MARCH, 2015

EXERGY AND ECONOMIC ANALYSES OF POLYMER ELECTROLYTE MEMBRANE (PEM) FUEL CELL SYSTEM CONFIGURATIONS

BY

Sani AYUBA, B.Eng. (ABU) 2009
MSc/ENG/7445/2011–2012

A THESIS SUBMITTED TO THE SCHOOL OF POSTGRADUATE STUDIES, AHMADU BELLO UNIVERSITY, ZARIA IN PARTIAL FULFILLMENT OF THE REQUIREMENTS FOR THE AWARD OF MASTER OF SCIENCE DEGREE IN CHEMICAL ENGINEERING

DEPARTMENT OF CHEMICAL ENGINEERING,
FACULTY OF ENGINEERING
AHMADU BELLO UNIVERSITY, ZARIA
NIGERIA

MARH, 2015

Declaration

I declare that the work in this Thesis titled ‘Exergy and Economic Analyses of Polymer Electrolyte Membrane (PEM) Fuel Cell System Configurations’ has been carried out by me in the Department of Chemical Engineering. The information derived from the literature has been duly acknowledged in the text and a list of references provided. No part of this thesis was previously presented for another degree or diploma at this or any other Institution.

Ayuba, Sani	Date

Certification

This Thesis entitled EXERGY AND ECONOMIC ANALYSES OF POLYMER ELECTROLYTE MEMBRANE (PEM) FUEL CELL SYSTEM CONFIGURATIONS by Sani AYUBA meets the regulations governing the award of Master of Science Degree of the Ahmadu Bello University, and is approved for its contribution to knowledge and literary presentation.

Dr. B. Mukhtar Chairman, Supervisory Committee	Date
Dr. S.M. Waziri Member, Supervisory Committee	Date
Dr. A.S. Olawale Member, Supervisory Committee	Date
Dr. S.M. Waziri Head of Department	Date
Prof. A.Z. Hassan Dean, School of Postgraduate Studies	Date

Acknowledgements

I give all thanks and praises to God for giving me the opportunity and enablement to execute this work.

I would like to express my utmost respect and sincere appreciation to my team of supervisors: Dr. B. Mukhtar, Dr. S.M. Waziri and Dr. A.S. Olawale. Without their keen supervision and invaluable guidance, insightful comments and encouragement, this work would not have been possible. Sirs, you all are wonderful!

I would also like to express my appreciation to my internal examiners for making good observations which contribute substantially to this work.

I would not forget to say a big thank you to EUtech Scientific Engineering GbmH, Germany, for providing me with the software – Thermolib, which was used in this work. I am very grateful. My appreciation also goes to all whose works have been cited in this work.

I would not also forget to say a big thank you to my uncle Barr. Yahaya Washiri for giving me all the financial and moral support I needed. What could I have done without you?

Abstract

One of the major problems facing commercialization of fuel cell systems, especially polymer electrolyte membrane (PEM) fuel cell systems is cost. Various researchers have reported different system configurations which perform differently in terms of energy utilization and cost. It is therefore important to determine the best system configuration in terms of both energy utilization and cost. In this work, exergy and economic analyses of five different PEM fuel cell system configurations were carried out in order to investigate the performance of the different systems. Thermolib software was used to simulate the operation of the systems in order to obtain data for the analysis. The return on investment (ROI) and payback period were used as measures of economic performance. The results indicated that the largest exergy loss occurs in the stack (over 90%) for all systems. This is due to the chemical exergy change that occurs as a result of the chemical change that takes place in the stack. System 1 showed the highest overall exergy and energy efficiencies of 30.18% and 59.48%, respectively followed by system 3 (29.32% and 57.79%), system 4 (28.35% and 55.88%), system 2 (26.14% and 51.52%) and system 5 (24.23% and 47.77%). An improved system configuration which has a hydrogen recirculation stream without blower and makes use of the compressor expander module (CEM) was proposed and also analyzed. It was found to have an overall exergy and energy efficiencies of 31.95% and 62.97%, respectively. The ROI and payback period evaluated for all five systems as well as the proposed system were: system 1 (3.8years and 20%), system 2 (9.4years and 4%), system 3 (4.3years and 16%), system 4 (5.8years and 11%), system 5 (12.7years and 1%) and the proposed system (2.9years and 27%). In term of both energy and cost, the proposed system configuration was found to have the best performance followed by system 1, system 3, system 4, system 2 and system 5, accordingly. This study has therefore established an improved PEM fuel cell system configuration.

Table of Contents

Declaration iii

Certification iv

Acknowledgements v

Abstract vi

Table of Contents vii

List of Figures x

List of Tables xii

Symbols and Abbreviations xiii

CHAPTER ONE 1

INTRODUCTION 1

1.1 Background to the Study 1

1.2 Problem Statement 3

1.3 Justification 3

1.4 Aim and Objectives 4

1.5 Scope 4

CHAPTER TWO 5

LITERATURE REVIEW 5

2.1 Basics of Fuel Cells 5

2.2 Types of Fuel Cells 6

2.2.1 PEM fuel cells 9
2.3 Thermodynamics of Fuel Cells 12
2.3.1 Fuel cell efficiency 14
2.3.2 Fuel cell voltage 16
2.4 Exergy Analysis 17
2.4.1 Comparison of energy and exergy analyses 20
2.4.2 Different forms of exergy 21
2.5 Simulation Software 24
2.5.1 Thermolib software 25
2.6 Related Works 26
CHAPTER THREE 30
METHODOLOGY 30
3.1 Modelling and Simulation of Selected PEM Fuel Cell System Configurations 30
3.2 Exergy Analysis 38
3.2.1 Evaluation of irreversibilities 38
3.2.2 Overall system exergy and energy efficiency 39
3.3 System Proposition 39
3.4 Economic Analysis 40
3.4.1 Cost estimation 40
3.4.2 Economic indicators 43
CHAPTER FOUR 45

RESULTS AND DISCUSSIONS OF RESULTS 45

4.1 Simulation Results 45

4.2 Exergy Analysis Results 46

4.3 System Proposition Results 55

4.4 Economic Analysis Results 55

CHAPTER FIVE 59

CONCLUSIONS AND RECOMMENDATIONS 59

5.1 Conclusions 59

5.2 Recommendations 60

REFERENCES 61

Appendix A: Thermolib Models of Systems 66

Appendix B: Stream Properties Obtained by Simulation 72

Appendix C: Cost Estimates and Economic Parameters 78

List of Figures

Figure 2.1: A schematic diagram of two dimensional sectional views of a fuel cell 6

Figure 2.2: Schematic diagram of a fuel cell system 11

Figure 2.3: Basic fuel cell inputs and outputs 12

Figure 2.4: Polarization curve showing voltage losses 17

Figure 2.5: Exergy of a low grade energy 19

Figure 3.1: System 1 (PEMFCS with air humidification only) 30

Figure 3.2: System 2 (PEMFCS with anode and cathode exit condensers) 31

Figure 3.3: System 3 (PEMFCS with anode and cathode pre – heaters) 32

Figure 3.4: System 4 (PEMFCS with enthalpy wheel and membrane humidifiers) 33

Figure 3.5: System 5 (PEMFCS with separate water source) 34

Figure 3.6: Zoomed section showing stream properties 37

Figure 4.1: Simulation results 45

Figure 4.2: Irreversibilities of system 1 components 46

Figure 4.3: Exergy efficiencies of system 1 components 46

Figure 4.4: Irreversibilities of system 2 components 48

Figure 4.5: Exergy efficiencies of system 2 components 48

Figure 4.6: Irreversibilities of system 3 components 49

Figure 4.7: Exergy efficiencies of system 3 components 49

Figure 4.8: Irreversibilities of system 4 components 50

Figure 4.9: Exergy efficiencies of system 4 components 50

Figure 4.10: Irreversibilties of system 5 components 51

Figure 4.11: Exergy efficiencies of system 5 components 51

Figure 4.12: Irreversibilities of proposed system components 52

Figure 4.13: Exergy efficiencies of proposed system components 52

Figure 4.14: Overall exergy and energy efficiencies of each system 53

Figure 4.15: Net power produced by each system 54

Figure 4.16: Fuel consumption of each system 54

Figure 4.17: Proposed System Configuration 55

Figure 4.18: Estimated costs of each system 56

Figure 4.19: Estimated costs of each system based on net power 56

Figure 4.20: Systems economic indicators 57

Figure A1: Thermolib model of system 1 66

Figure A2: Thermolib model of system 2 67

Figure A3: Thermolib model of system 3 68

Figure A4: Thermolib model of system 4 69

Figure A5: Thermolib model of system 5 70

Figure A6: Thermolib model of the proposed system 71

List of Tables

Table 2.1: Types of fuel cells 8

Table 2.2: Types of fuel cells and electrochemical reactions 9

Table 3.1: Components and distinct features of selected system configurations 35

Table 3.2: Specified system components data for simulation 37

Table 3.3: Capital cost parameters for the fuel cell stack 41

Table 3.4: Values of economic parameters 42

Table 3.5: Costs estimates in 2009 and 2014 43

Table B1: Stream properties of system 1 72

Table B2: Stream properties of system 2 73

Table B3: Stream properties of system 3 74

Table B4: Stream properties of system 4 75

Table B5: Stream properties of system 5 76

Table B6: Stream properties of proposed system configuration 77

Table C1: Systems and equipment costs estimates 78

Table C2: Economic analysis results 79

Symbols and Abbreviations

c	specific heat capacity (J/kg.K)
c_p	specific heat capacity at constant pressure (J/kg.K)
$\dot{E}_x$	exergy transfer rate (W)
$\dot{E}_{x,w}$	exergy transfer rate by work (W)
$\dot{E}_{x,Q}$	exergy transfer rate by heat (W)
$\dot{E}_x^{ch}$	chemical exergy rate (W)
$\dot{E}_x^{ph}$	physical exergy rate (W)
$\dot{E}_x^{ke}$	kinetic exergy rate (W)
$\dot{E}_x^{p}$	potential exergy rate (W)
$\dot{E}_x^{pe}$	thermo mechanical exergy rate (W)
E^o	standard potential (V)
f_i	total molar flow of stream i (mol/sec)
F	Faraday constant (C/mol)
$\bar{g}$	specific or molar Gibbs free energy (J/mol)
ΔG_r	Gibb's free energy change of reaction (J)
h	specific enthalpy (J/mol)
h_o	standard specific enthalpy (J/mol)
$h_{o,i}$	specific enthalpy of stream i at reference conditions (J/mol)
h_i	specific enthalpy of stream i at operating conditions (J/mol)
HHV	higher heating value (J)
$\dot{m}$	mass flow rate of stream (kg/sec)
N	number of electrons transferred
P	pressure (Pa)

P_o	standard pressure (Pa)
$\dot{Q}$	heat transfer rate (W)
R	gas constant (J/mol.K)
s	specific entropy (J/K)
s_o	standard specific entropy (J/K)
$s_{o,i}$	specific entropy of stream i at reference conditions (J/K)
s_i	specific entropy of stream i at operating conditions (J/K)
T	absolute temperature (K)
T_o	standard temperature (K)
V_{cell}	cell voltage (V)
V_{ohm}	ohmic losses (V)
V_{act}	acivation losses (V)
V_{conc}	concentration losses (V)
v_o	stream speed (m/sec)
v_m	specific volume (m^3/kg)
$\dot{W}$	work transfer rate (W)
$W_{sh,max}$	maximum shaft wok (J)
Z_o	stream altitude (m)
ψ	total specific exergy (J/mol)
ψ_{ph}	specific physical exergy (J/mol)
ψ_{ch}	specific chemical exergy (J/mol)
$x_{k,i}$	mole fraction of component k, in stream i
ψ_i	total specific exergy of stream i (J/mol)
$\psi_{ph,i}$	specific physical exergy of stream i (J/mol)
$\psi_{ch,i}$	specific chemical exergy of stream i (J/mol)

$\psi^{o}_{ch,k,i}$	standard specific chemical exergy of component k in stream i (J/mol)
η	energy efficiency (%)
η_{max}	maximum energy efficiency (%)
η_{II}	second law efficiency (%)

CHAPTER ONE

INTRODUCTION

1.1 Background to the Study

Fuel cells are electrochemical devices that directly convert chemical energy stored in fuels such as hydrogen, methanol, natural gas, etc to electrical energy. They have the potential to reduce the amount of pollutant emissions and dependence on fossil fuels. Due to the growing concerns on the depletion of petroleum based energy resources and climate change; fuel cell technologies have received much attention in recent years owing to their high efficiencies and low emissions. There are different types of fuel cells and are classified according to the electrolyte employed. The polymer electrolyte membrane (PEM) fuel cell also known as proton exchange membrane fuel cell uses a proton conductive polymer membrane electrolyte. PEM fuel cell technology has drawn the most attention in recent years because of its simplicity, viability, and it has been demonstrated in almost any conceivable application from powering a cell phone to a locomotive (Barbir, 2005). However, the most important application is in transportation and stationary power generation.

Compared to the internal combustion engines (ICEs), fuel cells have several advantages. The main advantages are high efficiency and low emissions. They are 2 – 3 times more efficient than ICEs (Thomas and Zalbowitz, 2000). Fuel cells directly convert fuel energy into electrical energy, whereas ICEs convert the fuel energy to thermal energy first, then to mechanical energy. Due to the thermal energy involved, the ICE conversion of energy is limited by the Carnot Cycle. This is not the case with fuel cells. Fuel cells are considered zero emission power generators if pure hydrogen from a clean source is used as fuel.

The efficiency of fuel cells is one of the primary benefits of the technology. Although this is true in principle, it is important to distinguish between fuel cell stack efficiency and fuel cell system efficiency: Fuel cell stack efficiency is commonly taken to mean the actual efficiency of the electrochemical reaction whereas fuel cell system efficiency relates to the overall performance of the fuel cell system. A fuel cell stack can only operate if provided with other equipment, which unfortunately introduce losses and reduce the total efficiency of the system.

The conversion efficiency is the most important factor in an energy system. In order to analyze the system, each unit of the system should be carefully analyzed and the quality of energy should be considered. The most commonly used method for analysis of energy systems is the first law of thermodynamics. However a modern approach to process analysis uses exergy analysis, which provides a more realistic view of the process and a useful tool for engineering evaluation (Nuhu *et al.*, 2012).

The exergy concept is used for the evaluation of the system considering the irreversibility. The exergy is often called the available energy. Exergy analysis is an effective method using the conservation of mass and energy principles together with the second law for the design and analysis of energy systems, and a way to study how systems and processes can be made more efficient by determining the locations, types, and true magnitudes of energy wastes and losses. It is an efficient technique that reveals whether or not and by how much it is possible to design more efficient energy systems by reducing the inefficiencies. The exergy analysis is considered better than an enthalpy (energy) analysis because it can deal with the quality of energy and evaluate different forms of energy like chemical, thermal and electrical by a unified measure. In addition, the degree of irreversibility in each element of the system can be quantitatively discussed. Through exergy analysis, the units that have large exergy losses can easily be

found and guidelines provided for improving the conversion system. In this work, different PEM fuel cell system configurations were studied and an exergy and economic analyses of selected system configurations were carried out to determine the one that has the best performance in terms of both cost and energy utilization. An improved system configuration was also proposed.

1.2 Problem Statement

Fuel cells technology is an important emerging technology. However, one of the major problems facing commercialization of fuel cells, particularly PEM fuel cells is cost. Various researchers have designed different PEM fuel cell system configurations, which perform differently in terms of energy utilization and cost. It is therefore important to determine the system configuration that gives the best performance in terms of energy utilization and cost.

1.3 Justification

i. Generally, fuel cells have high energy conversion efficiency. However, a more energy efficient system configuration (in terms of number of components and their arrangements) is required in order to make them more attractive.

ii. Though very expensive, especially the PEM fuel cells, they are becoming very important as prices are falling due to intense research and development efforts going on globally. Therefore, having a more cost efficient fuel cell system configuration would further reduce the cost of PEM fuel cell systems.

iii. There are lots of research and development of fuel cells technology going on worldwide so it is important for Nigeria to also participate to acquire the know-how.

1.4 Aim and Objectives

Aim: To determine the PEM fuel cell system configuration with the best performance in terms of energy utilization and cost through exergy and economic analyses.

Objectives

i. To study and select five different PEM fuel cell system configurations to be used for the analysis.
ii. To model and simulate the operation of the selected systems using Thermolib software.
iii. To carry out exergy and economic analyses to determine the system configuration with the best performance in terms of cost and energy utilization.
iv. To propose an improved system configuration.

1.5 Scope

The study is restricted to simulation of PEM fuel cell operation and exergy and economic analyses of PEM fuel cell system configurations.

CHAPTER TWO

LITERATURE REVIEW

2.1 Basics of Fuel Cells

Fuel cells are devices that convert chemical energy of a fuel into electrical energy through electrochemical processes. The main advantages of fuel cells are high energy conversion efficiency and low emission or near zero emission of pollutants. While the main disadvantages include high cost and lack of established fuel infrastructure.

Fuel cell technology is based upon the following simple electrochemical reactions (Thomas and Zalbowitz, 2000):

Anode reaction: $2H_2 \longrightarrow 4H^+ + 4e^-$ ……..... (2.1)

Cathode reaction: $O_2 + 4H^+ + 4e^- \longrightarrow 2H_2O$ …..……...…..… (2.2)

The overall reaction is: $2H_2 + O_2 \longrightarrow 2H_2O$ ……..……...…. (2.3)

The electrons produced can be harnessed to provide electricity in a consumable form through a simple circuit with a load. The phenomena involved in PEM fuel cell operation are complex; specifically, they involve heat transfer, species and charge transport, multi-phase flows, and the electrochemical reactions. In theory, a fuel cell will continuously produce electricity as long as fuel is supplied. The basic design of a fuel cell involves two electrodes on either sides of an electrolyte. Hydrogen and oxygen is passed over each of the electrodes and through means of an electrochemical reaction, electricity, heat and water are produced. This process is schematically shown in Figure 2.1.

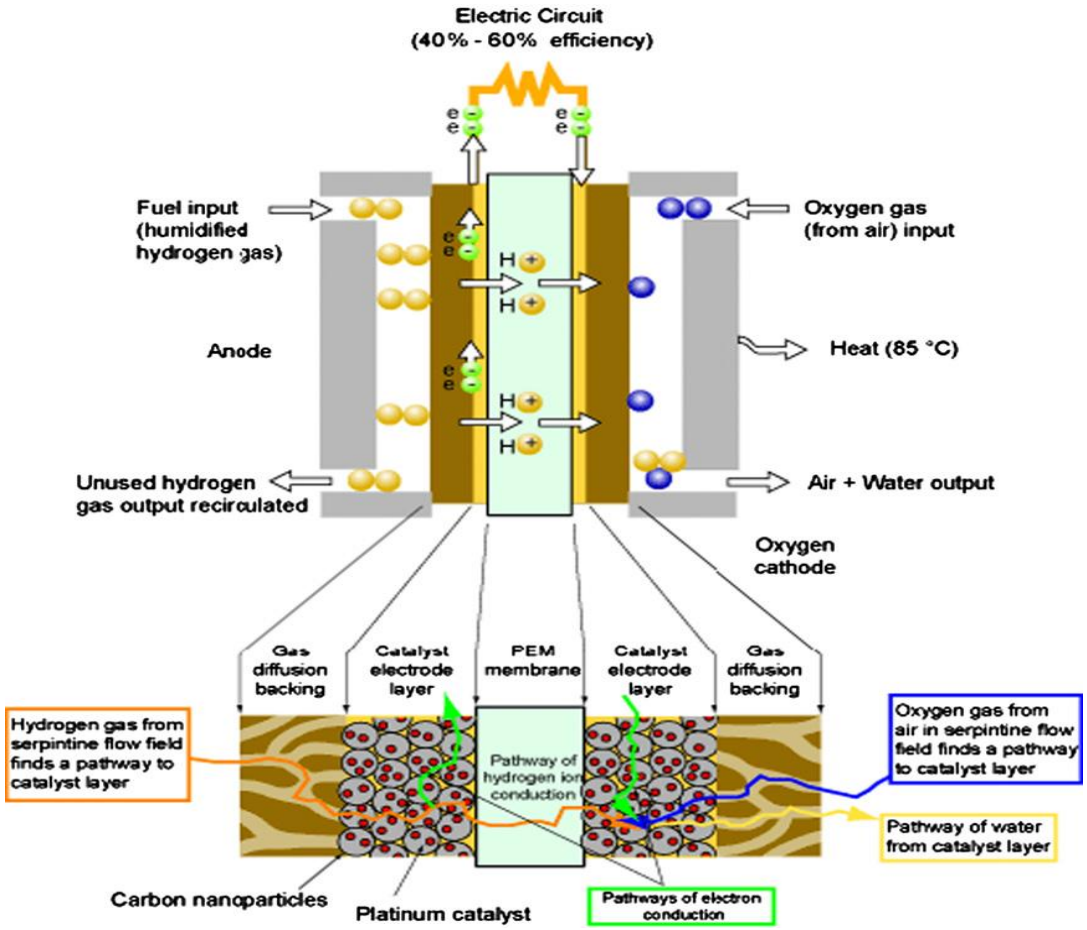


Figure 2.1: A schematic diagram of two dimensional sectional views of a fuel cell

Source: Wang *et al.* (2011)

The hydrogen fuel can be supplied from a variety of sources if a fuel reformer is added to the fuel cell system. Therefore, hydrogen can be obtained from hydrocarbon fuels such as natural gas or methanol.

2.2 Types of Fuel Cells

Fuel cells differ primarily by the type of fuel and electrolyte used. The type of electrolyte, in turn, determines the operating temperature, which varies widely among the different types. High temperature fuel cells operate above 600°C (600 – 1000°C). These high temperatures permit the spontaneous internal reforming of light hydrocarbon fuels such as methane into hydrogen and carbon in the presence of water. This reaction

occurs at the anode over a nickel catalyst provided that adequate heat is always available. This is essentially a steam reforming process.

Internal reforming eliminates the need for a separate fuel processor, and can use fuels other than pure hydrogen. These significant advantages could lead to an increase in overall efficiency by as much as 15%, (Lanz *et al*., 2001). During the electrochemical reaction that follows, the fuel cell draws on the chemical energy released during the reaction between hydrogen and oxygen to form water, and the reaction between carbon monoxide and oxygen to form carbon dioxide.

High temperature fuel cells also generate high – grade waste heat, which can be used in downstream processes for cogeneration purposes. High temperature fuel cells react easily and efficiently without an expensive noble metal catalyst, such as platinum. On the other hand, the amount of energy released by the electrochemical reaction degrades as the reaction temperature increases perhaps due to increase in electrical resistance and materials degradation. High temperature fuel cells suffer from severe materials problems. Few materials can work for extended periods without degradation within a chemical environment at high temperature. Furthermore, high temperature operation does not lend itself easily to large scale operations and is not suitable where quick startup is required. As a result, current high temperature fuel cells applications have focused on stationary power plants where the efficiencies of internal reforming and co– generative capabilities outweigh the disadvantages of material breakdown and slow startup. The most prominent high temperature fuel cells are:

i. Molten Carbonate Fuel Cell (MCFC)
ii. Solid Oxide Fuel Cell (SOFC).

Low temperature fuel cells typically operate below 250ºC (50 – 200ºC). These low temperatures do not permit internal reforming, and therefore require an external

source of hydrogen. On the other hand, they exhibit quick startup, suffer fewer materials problems and are easier to handle in vehicle applications. The most prominent low – temperature fuel cells are:

i. Alkaline Fuel Cell (AFC),

ii. Phosphoric Acid Fuel Cell (PAFC),

iii. Polymer Electrolyte Membrane Fuel Cell (PEMFC),

iv. Direct Methanol Fuel Cell (DMFC).

Table 2.1 shows classification of the different types of fuel cells.

Table 2.1: Types of fuel cells

Fuel Cell Type	**Operating Temperature (°C)**	**System Power Output**	**Application**
PEMFC	50-100	1kW – 500kW	Backup power, portable power, transportation, small distributed power generation
DMFC	60-90	1W – 100W	Small portable power devices
AFC	90-100	10kW –100kW	Military and space
PAFC	150-200	50kW – 1MW	Distributed power generation
MCFC	600-700	1kW – 1MW	Large distributed power generation and electric utility.
SOFC	600-1000	1kW – 3MW	Auxiliary power, large distributed power generation and electric utility

Source: Sanghai (2013)

Table 2.2 shows the electrochemical reactions that take place in the different types of fuel cells.

Table 2.2: Types of fuel cells and electrochemical reactions

Fuel Cell Type	Anode reaction	Cathode reaction	Overall reaction
PEMFC	$H_2 \rightarrow 2H^+ + 2e^-$	$1/2O_2 + 2H^+ + 2e^- \rightarrow H_2O$	$H_2 + 1/2O_2 \rightarrow H_2O$
DMFC	$CH_3OH + H_2O \rightarrow CO_2 + 6H^+ + 6e^-$	$3/2O_2 + 6H^+ + 6e^- \rightarrow 3H_2O$	$CH_3OH + 3/2O_2 \rightarrow 2H_2O + CO_2$
AFC	$H_2 + 2OH^- \rightarrow 2H_2O + 2e^-$	$1/2O_2 + H_2O + 2e^- \rightarrow 2OH^-$	$H_2 + 1/2O_2 \rightarrow H_2O$
PAFC	$H_2 \rightarrow 2H^+ + 2e^-$	$1/2O_2 + 2H^+ + 2e^- \rightarrow H_2O$	$H_2 + 1/2O_2 \rightarrow H_2O$
MCFC	$H_2 + CO_3^{2-} \rightarrow H_2O + CO_2 + 2e^-$	$1/2O_2 + CO_2 + 2e^- \rightarrow CO_3^{2-}$	$H_2 + 1/2O_2 \rightarrow H_2O$
SOFC	$H_2 + O^{2-} \rightarrow H_2O + 2e^-$	$1/2O_2 + 2e^- \rightarrow O^{2-}$	$H_2 + 1/2O_2 \rightarrow H_2O$

Source: Sanghai (2013)

2.2.1 PEM fuel cells

PEM fuels cell technology is the most promising for automotive propulsion because of its simplicity, high efficiency, and quick – start up (Barbir *et al.*, 1999). The critical component of a PEM fuel cell is obviously the membrane that is impermeable to the reactant gases and conducts protons. The electrolyte is composed of a solid polymer film that consists of a form of acidified Teflon.

A fuel cell stack consists of a number of single cells stacked up so that the cathode of one cell is electrically connected to the anode of the adjacent cell. In this way exactly the same current passes through each of the cells. Physically, each fuel cell consists of a membrane electrode assembly (MEA), which consists of the anode, cathode, electrolyte and catalyst, sandwiched between two flow field plates made of graphite. The plates channel the fuel and air to opposite sides of the MEA. Coolant is used to regulate the fuel cell reaction temperature. To facilitate this, cooling plates are placed between each fuel cell. These cooling plates channel the coolant past the fuel cells to absorb or supply heat as required. Seals between the graphite plates ensure that the oxidant, fuel and coolant streams never mix within the fuel cells. Electrical

endplates are placed at either end of the series of flow field plates. These endplates are connected to the terminals from which the output power is drawn, and typically include the fluid and gas interface connections. The entire sequence of plates is held together by a series of tie rods or other mechanical means (Lanz *et al*., 2001).

Humidification of the reactant gases is an important aspect of PEM fuel cell operation. Adequate humidification is required to ensure ion conduction and prevent fuel cell damage. The amount of water that a gas can absorb is highly dependent on the humidification temperature particularly at low pressure. Since hotter gases can hold more water than colder gases, the gases must be humidified at or near the fuel cell operating temperature (as set by the stack coolant temperature). In some fuel cell systems, humidifiers are integrated into the stack itself while in others they are separate external components (Lanz *et al*., 2001).

Practical fuel cell design focuses on achieving a high power output per area of membrane, scaling the active membrane area to a useful size, and making the overall stack suitably compact for its intended use. Critical areas of concern are seals, flow field pattern tolerances and cell alignment. As with any commercial product, the resulting design must be reliable, manufacturable, and economically viable and have a significant operating life. The fuel cell stack is obviously the heart of a fuel cell system; however, without the supporting equipment the stack itself would not be very useful. The fuel cell system typically involves the following subsystems (Barbir, 2005).

i. Oxidant supply (oxygen or air)
ii. Fuel supply (hydrogen or hydrogen-rich gas)
iii. Heat management
iv. Water management
v. Power conditioning
vi. Instrumentation and controls.

The system configuration greatly depends on the application. In some cases a very simple system consisting of nothing more than a bottle of hydrogen and a fuel cell may be sufficient. In other cases the system needs a number of components and the subsystems. Figure 2.2 shows a schematic diagram of an actual hydrogen – air fuel cell system. In order to circumvent the issue of hydrogen availability and infrastructure, a fuel cell may be integrated with a fuel processor allowing hydrogen generation from hydrocarbon fuels, such as natural gas, gasoline or methanol.

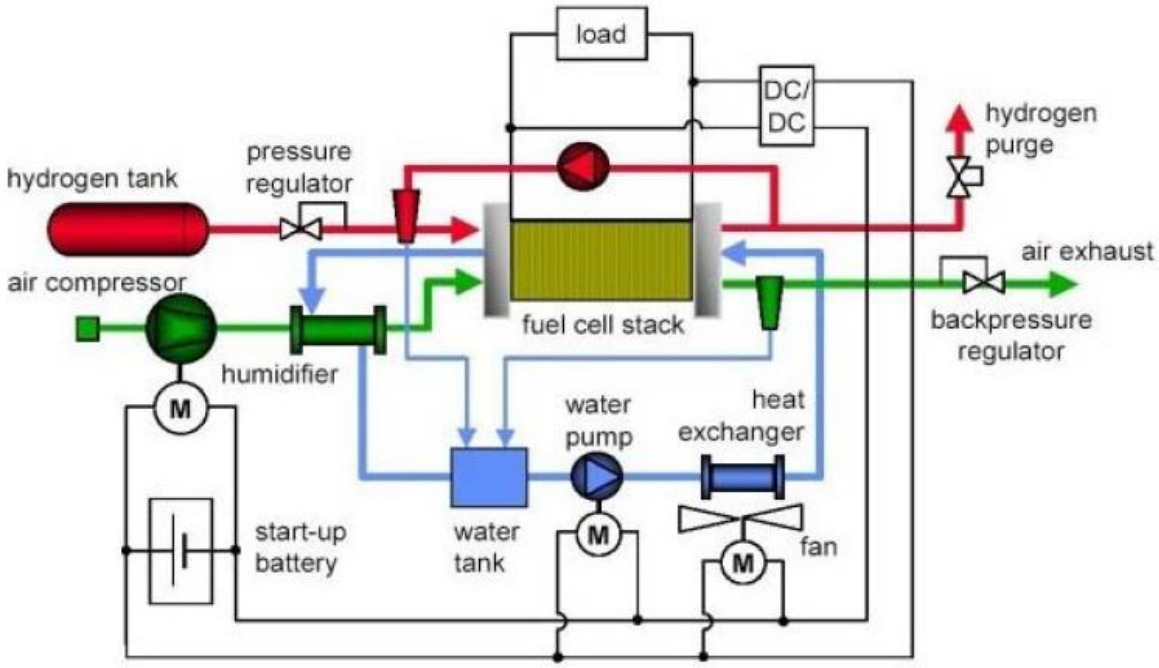


Figure 2.2: Schematic diagram of a fuel cell system
Source: Barbir (2005)

Hydrogen can be generated from hydrocarbon fuels by several processes, such as:

- Steam reformation
- Partial oxidation
- Autothermal reformation, which is essentially a combination of steam reformation and partial oxidation.

In addition, several other processes must be employed in order to produce hydrogen pure enough to be used in PEM fuel cells, such as:

- Desulfurization – to remove sulfur compounds present in fuel
- Shift reaction – to reduce the content of CO in the gas produced by the fuel processor
- Gas cleanup, involving preferential oxidation, methanation and/or membrane separation – to further minimize the CO content in the reformate gas.

The reforming process needs water and air and thermal management.

2.3 Thermodynamics of Fuel Cells

Fuel cells are electrical power generating systems. They convert chemical energy into electrical energy by electrochemical reactions. The inputs and outputs of a basic fuel cell are shown in Figure 2.3. The basic energy conversion of a fuel cell is described as:

Chemical energy of fuel = Electrical energy + Heat energy

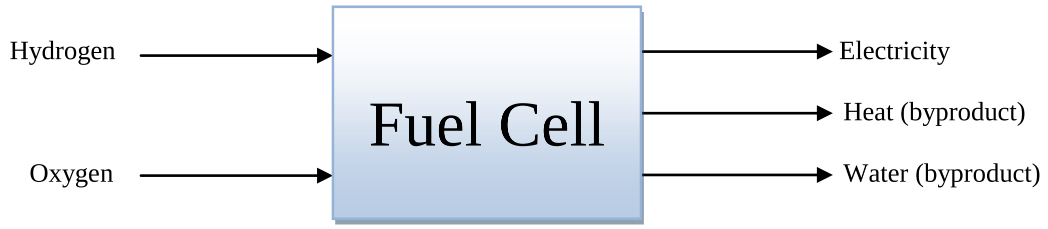


Figure 2.3: Basic fuel cell inputs and outputs

The above energy balance is described in more detail using the first and second laws of thermodynamics as follows:

The mathematical statement of the first law of thermodynamics applied to the fuel cell (Thermodynamics of Fuel Cells, n.d.) is:

$$\Delta H = Q - NFE \qquad (2.4)$$

where N = number of electrons transferred

F = Faraday’s constant and

E = cell potential or voltage

The mathematical statement of the second law of thermodynamics is:

$$\Delta S_{total} = \Delta S_{system} + \Delta S_{surroundings} \geq 0 \text{ ....} \quad (2.5)$$

where equality applies for reversible processes and inequality applies for irreversible processes.

For a process undergoing reversible heat transfer, Q_{rev} at a constant temperature T_o,

$$\Delta S = \frac{Q_{rev}}{T_o} \quad (2.6)$$

If we consider the fuel cell to be ideal, meaning that it is reversible and thus behaves as a perfect electrochemical apparatus, combining first and the second laws of thermodynamics for a reversible process, from Equation (2.6) gives:

$$\Delta H = T\Delta S - NFE \quad (2.7)$$

Writing Equation (2.7) in a differential form:

$$dH = TdS - FEdN \quad (2.8)$$

Since the cell is operating reversibly, the losses are minimum and the useful work obtained is maximum. This work is very significant and is represented by the Gibbs free energy:

$$dG = -FEd \quad (2.9)$$

Substituting Equation (2.9) in Equation (2.8) gives:

$$dG = dH - TdS \quad (2.10)$$

This is the thermodynamic expression for the maximum useful work obtainable from a system.

H represents the total energy of the system, and S represents the "unavailable" energy (that which cannot be converted to useful work).

The electrons released to generate the electrical work are, of course, inherently related to the electrochemical reaction taking place. So ΔG can also be associated with the chemical energy released during the electrochemical reaction occurring in the fuel cell. Typically, a "free energy of formation", ΔG_f or ΔG^o is computed for these

reactions, where the free energy is referenced with respect to standard temperature and pressure (s.t.p.) conditions.

For a given reaction:

$$\Delta G^{o} = \Delta G^{o}_{products} - \Delta G^{o}_{reactants} \quad \text{..... (2.11)}$$

The reversible open circuit voltage (i.e. maximum voltage that could be generated) can be calculated based on ΔG^{o} as:

$$E^{o} = \frac{-\Delta G^{o}}{NF} \quad \text{..... (2.12)}$$

2.3.1 Fuel cell efficiency

Fuel cell efficiency cannot be analyzed the same way as a thermodynamic system using the Carnot efficiency because it is independent of the Carnot cycle. It is determined by the Gibbs free energy, ΔG, and the enthalpy of formation", ΔH. The "enthalpy of formation" is the value given to the heat that would be produced by burning the fuel. The enthalpy of formation is more commonly referred to as the calorific value. The efficiency of a fuel cell is given by:

$$\frac{\text{Electrical energy produced}}{-\Delta H} = \frac{\Delta G}{\Delta H} \quad \text{..... (2.13)}$$

The efficiency equation, (Equation 2.13), can be ambiguous in that the enthalpy of formation depends on the state of the water product in the governing combustion equation. The product water can be in the form of either steam or liquid. For the product water in the form of steam being produced, the specific enthalpy of formation is, ΔH = −241.83kJ/mole, whereas, for water in the form of liquid being produced, ΔH = −285.84kJ/mole (Rayment and Sherwin, 2003). The difference between the two enthalpies of formation values is due to the molar enthalpy of vaporization of water. The enthalpy of formation corresponding to the water in the liquid state is known as the higher heating value (HHV) whereas the enthalpy of formation corresponding to the

water in the vapour state is known as the lower heating value (LHV). The heating value is a common term applied to a fuel, and it is a positive number equal to the enthalpy of combustion. The higher heating value is the value given when the product of the combustion is a liquid and the lower heating value is the value corresponding to when the product is in the gas form (Rayment and Sherwin, 2003).

The fuel cell efficiency (first law) is expressed as:

$$\eta = \frac{W_{out}}{Q_{in}} \quad \text{(2.14)}$$

The work done (W) is given by − ΔG or (NFE) and the heat input (Q) is calculated based upon the higher heating value (HHV) of the fuel.

$$\eta = \frac{-\Delta G}{HHV} = \frac{NFE}{HHV} \quad \text{(2.15)}$$

The maximum efficiency (first law) occurs at standard conditions – highest possible cell voltage:

$$\eta_{max} = \frac{\Delta G^o}{HHV} = \frac{NFE^o}{HHV} \quad \text{(2.16)}$$

For a typical H_2/O_2 fuel cell, the maximum efficiency calculated from Equation (2.16) is approximately 83%. A Carnot engine would have to have a high temperature of 1753K (with a corresponding low temperature of 298K) to achieve this efficiency! The maximum efficiency (first law) from Equation (2.16) is quite meaningless from a practical standpoint (Rayment and Sherwin, 2003). This is because no current is being drawn (open circuit conditions). Therein lies the limitation of the efficiencies predicted by the first law. This can be redressed by using the practical efficiency (second law). This indicates the actual work obtained to the maximum work obtainable:

$$\eta_{II} = \frac{NFV_{cell}}{NFE^o} = \frac{V_{cell}}{E^o} \quad \text{(2.17)}$$

2.3.2 Fuel cell voltage

The standard potential E^o is a quantitative measurement of the maximum cell potential, i.e., the open circuit voltage. For a hydrogen − oxygen fuel cell, in which there is a transfer of two electrons for each water molecule, $E^o = 1.229V$ if the produced water is in liquid state and $E^o = 1.18V$ if the produced water is in gaseous state (Basualdo *et al*., 2012). These values correspond to normalized conditions: cell temperature equal to 298.5K and partial pressures of oxygen and hydrogen equal to 1 atm. However, in practice the cell potential is significantly lower than the theoretical potential because there are some losses even when no external load is connected. Moreover, when a load is connected to the fuel cell the voltage in the terminals decreases still more due to a number of factors, including polarization losses and interconnection losses between cells. The main voltage losses in a fuel cell are the following (Basualdo *et al*., 2012):

i. Activation loss: The activation losses, V_{act} are caused by the slowness of the reaction that takes place on the surface of the electrodes. A proportion of the generated voltage is lost in maintaining the electrochemical reaction that transfers electrons from the anode towards the cathode. This phenomenon is strongly nonlinear, and more important, it is at low current densities.

ii. Fuel crossover and internal currents: These energy losses result from the waste of fuel passing through the electrolyte and from electron conduction through the electrolyte. In PEMFC, the fuel losses and internal current are small and their effects are usually negligible.

iii. Ohmic loss: The ohmic losses, V_{ohm} are caused by the resistance to the transport of electrons through the electrodes and the different interconnections, and also to

the passage of ions through the electrolyte. The behavior of V_{ohm} is approximately linear with the current density.

iv. Concentration loss: The concentration losses, V_{conc} are caused by the diffusion of ions through the electrolyte which produces an increase in the concentration gradient, diminishing the speed of transport. The relation between the voltage of the cell and the current density is approximately linear up to a limit value, beyond which the losses grow quickly.

Therefore, the fuel cell voltage, V_{cell} of a single cell can be expressed as:

$$V_{cell} = E^o - V_{ohm} - V_{act} - V_{conc} \quad \text{..... (2.18)}$$

A typical polarization curve showing the potential and power density as a function of the current density is shown in Figure 2.4.

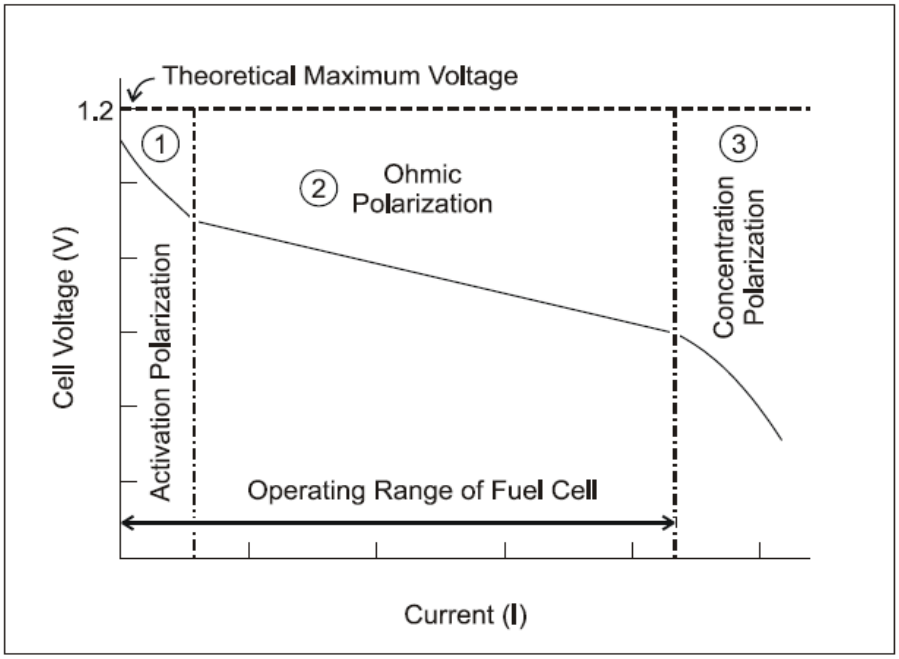


Figure 2.4: Polarization curve showing voltage losses
Source: Lanz *et al*. (2001)

2.4 Exergy Analysis

First law of thermodynamics gives the two different status of energy: point function status and path function status. Heat and work are identified as path function energies which are only defined in transit between the system and surrounding. But

there are energies with point function property which can be stored within the system and are ascribed as the system properties and therefore they are point functions. These are internal energies. First law tells that the difference between the heat and work interaction in a process is that energy which is stored in a system which gives status of point function. So, first law of thermodynamics gives birth to two status of energy as point function and path function but second law gives a directional constraint as far as the mutual convertibility between heat and work in a continual cyclic process is concerned. It states that heat can never be converted completely into work continuously in a cyclic process; what so ever the cyclic process may be. Even in an ideal case it cannot be done. But work can be continuously converted into an equal amount of heat.

This is the basic foundation on which the two grades of energy – High grade energy and low grade energy are defined. High grade energy is that energy which can be continuously converted into low grade energy but low grade energy is that energy which cannot be continuously converted into high grade energy. This is the reason that work is defined as high grade energy whereas heat is defined as low grade energy. Aside the mechanical form of internal energy is the intermolecular energy which is due to the temperature of the system, chemical bond energy of the system; these energies stored within the system as point function are also termed as low grade energies because they cannot be fully converted into useful work. This is further illustrated in Figure 2.5.

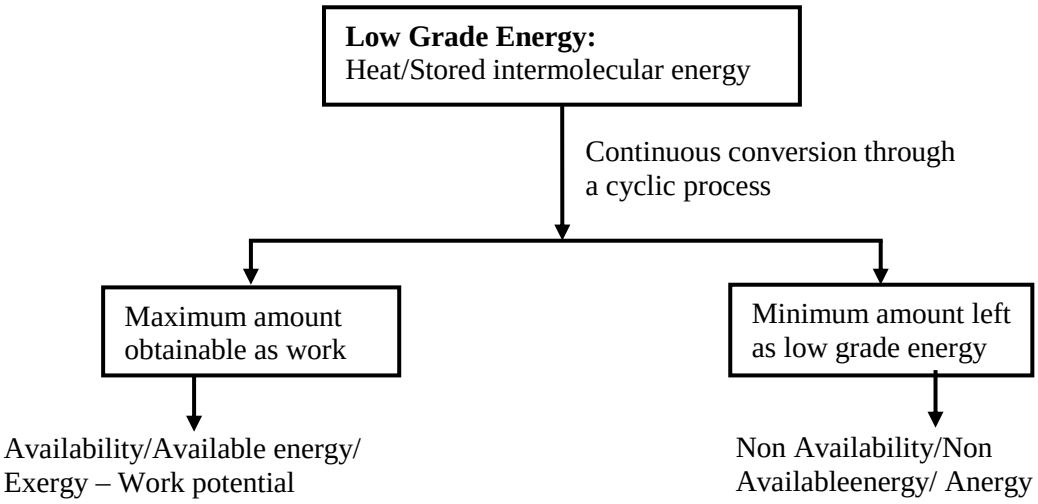


Figure 2.5: Exergy of a low grade energy

From Figure 2.5 it is shown that given a system of low grade energy, if this is to be converted (continuous conversion through a cyclic process) into useful work, a maximum amount is obtainable as work. This is called the Availability/ Available energy or Exergy and sometimes the work potential of the system. A minimum amount will be left as low grade energy. This is called the non Availability/ non Available energy or Anergy of the system. It should be noted that the exergy of a system depends not only on the state of the system but also the environment.

The exergy of a system is the maximum work obtainable as the system interacts and comes to equilibrium with the surrounding. The first law analysis did not give information on heat availability at different temperatures. It is the second law which asserts that from engineering perspective. Therefore, exergy method is a technique based on both the first and second laws of thermodynamics providing the locations where the exergy destruction and irreversibility are most. Ways and means can then be explored to reduce these exergy destructions to the practical minimum values.

The exergy destruction is a measure of thermodynamic inefficiency of a process and is expressed in terms of lost work potential. In general, the expression for exergy destruction rate as articulated by (Kotas, 2004) is:

$$\dot{I} = T_o\left[\left(\dot{S}_{out} - \dot{S}_{in}\right) - \sum_{i=1}^{n}\frac{\dot{Q}_i}{T_i}\right] = T_o\dot{S}_G \geq 0 \quad \text{..... (2.19)}$$

where $\dot{I}$ is the exergy destruction rate, $\dot{S}_{in}$, $\dot{S}_{out}$ and $\dot{S}_G$ are the entropy flow in and out of system and rate of entropy generation, respectively, $\dot{Q}_i$ is the rate of heat transfer at the location on the boundary where the temperature is T_i.

2.4.1 Comparison of energy and exergy analyses

The energy balance is the basic method of process investigation. It makes the energy analysis possible, points at the needs to improve the process, is the key to optimization and is also the basis for developing the exergy balance (Vosough *et al.*, 2011). Analysis of the energy balance results would disclose the efficiency of energy utilization in particular parts of the process and allow comparing the efficiency and the process parameters with the currently achievable values in the most modern installations. They will establish also the priority of the processes requiring consideration, either because of their excessive energy consumption or because of their particularly low efficiency (Vosough *et al.*, 2011). However, the energy approach has some deficiencies. The energy analysis is not able to recognize different quality of energy, (e.g., 1MW of heat equals 1MW of electricity). Accordingly, the energy analysis does not recognize the heat quality, which however depends on the heat source temperature, e.g., a 100kJ of heat at 1000°C is dramatically more valuable than the 100kJ of heat at the 50°C level because of its exergy or the work that can deliver. The energy analysis is blind for the process direction, and, e.g., will not indicate any error considering a 100kJ of heat at 5°C conducted through a partition to an environment at 100°C (Vosough *et al.*, 2011).

For these reasons the modern approach to the process analysis uses the exergy analysis, which provides a more realistic view of the process. The exergy analysis is the modern thermodynamic method used as an advanced tool for engineering process

evaluation. Whereas the energy analysis is based on the first law of thermodynamics, the exergy analysis is based on both the first and the second laws of thermodynamics. Both analyses utilize also the material balance for the considered system. Analysis and optimization of any physical or chemical process, using the energy and exergy concepts, can provide the two different views of the considered process. The exergy concept was introduced to overcome the limitations of the energy analysis.

2.4.2 Different forms of exergy

I. Work exergy

Exergy is defined as the maximum useful work potential of a system. Therefore, a work interaction in energy terms is equivalent in exergy terms. This means that the exergy transfer rate of a work flow, $\dot{E}_{x,w}$ equals the amount of work of the flow, $\dot{W}$:

$$\dot{E}_{x,w} = \dot{W} \quad \text{..... (2.20)}$$

For expansion work in a piston – cylinder device, part of the work is used to push the atmosphere away when the system expands and so cannot be further utilized. Thus, the exergy transfer rate by expansion work equals the difference between the expansion work and the surroundings work as represented by Equation (2.21).

$$\dot{E}_{x,w} = \dot{W} - P_o \frac{dV}{dt} \quad \text{..... (2.21)}$$

II. Heat transfer exergy

Assuming a uniform temperature distribution in a thermal energy reservoir, the exergy transfer rate, $\dot{E}_x$, connected with the heat transfer rate, $\dot{Q}$, can be calculated by the following formula:

$$\dot{E}_{x,Q} = \dot{Q}\left(1 - \frac{T_o}{T}\right) \quad \text{..... (2.22)}$$

where T_o is the ambient temperature, which is set to 298K and T is the heat source temperature.

III. Steady state stream flow exergy

Exergy transfer rate associated with material streams can be calculated with the following formula (Vosough *et al.*, 2011):

$$\dot{E}_x = \dot{E}_x^{ph} + \dot{E}_x^{ch} \quad \text{..... (2.23)}$$

$$\dot{E}_x^{ph} = \dot{E}_x^{ke} + \dot{E}_x^{p} + \dot{E}_x^{pe} \quad \text{..... (2.24)}$$

where

$\dot{E}_x^{ke} = \frac{1}{2}\dot{m}v_o^2$ represents the kinetic exergy rate, where v_o is the speed of the stream flow relative to the earth surface. $\dot{E}_x^{p} = \dot{m}gZ_o$ presents the potential exergy rate, where g is the earth's gravity and Z_o the stream altitude above sea level. $\dot{E}_x^{pe}$ represents the thermo mechanical exergy rate based on the temperature and the pressure of the stream. $\dot{E}_x^{ch}$ represents the chemical exergy rate based on the chemical potentials of the components in the stream. The total specific exergy is written as:

$$\psi = \psi_{ph} + \psi_{ch} \quad \text{..... (2.25)}$$

where $\psi = \frac{\dot{E}_x}{\dot{m}}$

$\dot{m}$ is the mass flow rate of the stream.

IV. Physical exergy

Physical exergy, known also as thermo mechanical exergy, is the work obtainable by taking the substance through reversible process from its initial state (T, P) to the state of the environment (T_o, P_o). The specific physical exergy is written as (Vosough *et al.*, 2011):

$$\psi_{ph} = h - h_o - T_o(s - s_o) \quad \text{..... (2.26)}$$

where h and *s* are the specific or molar enthalpy and entropy at the actual temperature, T and pressure,P while h_o and s_o are the same properties at the temperature, T_o and pressure, P_o of the environment.

For a perfect gas with constant c_p,

$$\psi_{ph} = c_p T_o\left(\frac{T_1}{T_o} - 1 - \ln\frac{T_1}{T_o}\right) + RT_o \ln\frac{P_1}{P_o} \quad \text{(2.27)}$$

For solids and liquids when assuming a constant specific heat, c:

$$\psi_{ph} = c\left[(T - T_o) - T_o \ln\left(\frac{T}{T_o}\right)\right] - v_m(P - P_o) \quad \text{(2.28)}$$

where v_m is the specific volume determined at T_o.

V. Chemical exergy

Chemical exergy is equal to the maximum amount of work obtainable when the substance under consideration is brought from the environmental state to the dead state by processes involving heat transfer and exchange of substances only with the environment (Jafarmadar, 2012). The specific chemical exergy, ψ_{ch}, depends on the mole fraction of each species, x_i, in the system, their chemical potential at the restricted dead state (state of thermal and mechanical equilibrium), $\mu_i(T_o, P_o)$, and the chemical potential of each species at the true dead state (state of thermal, mechanical and chemical equilibrium) in the environment $\mu_{io}(T_o, P_o, x_{io})$:

$$\psi_{ch} = \sum x_i(\mu_i - \mu_{io}) \quad \text{(2.29)}$$

When a substance does not exist in the reference environment, it must first react to reference substances in order to get in equilibrium with the environment. The reaction exergy at reference conditions equals the standard Gibbs energy change. So the overall specific chemical exergy term (Vosough *et al.*, 2011) becomes:

$$\mu_i = \bar{g}(T_o, P_o) + RT_o \ln x_i \quad \text{(2.30)}$$

$$\mu_{io} = \bar{g}(T_o, P_o) + RT_o \ln x_{io} \quad \text{(2.31)}$$

The specific chemical exergy of a pure gas assuming ideal gas is given by:

$$\psi_{ch} = RT \ln\left(\frac{P}{P_i}\right) = -RT \ln(x_{io}) \quad \text{(2.32)}$$

The specific chemical exergy of an ideal gas mixture or a mixture of ideal liquids is given by (Jafarmadar, 2012):

$$\psi_{ch} = RT \sum x_i \ln\left(\frac{x_i}{x_{io}}\right) \ldots\ldots\ldots\ldots\ldots\ldots\ldots\ldots\ldots\ldots \quad (2.33)$$

For a gaseous stream flow, the molar chemical exergy of all species can be found using (Casas, 2010):

$$\psi_{ch} = \sum x_i \psi^{o}_{ch,i} + RT_o \sum x_i \ln x_i \ldots\ldots\ldots\ldots\ldots\ldots\ldots\ldots \quad (2.34)$$

For substances not present in environment, consider an idealized reaction of the substance with other substances (usually reference substances for which exergies are known) so that the final products also are reference substances (Chemical Exergy, n.d.):

$$C_a H_b + \left(a + \frac{b}{4}\right) O_2 \rightarrow aCO_2 + \frac{b}{2} H_2O \ldots\ldots\ldots\ldots\ldots\ldots\ldots\ldots \quad (2.35)$$

Assuming no irreversibility,

$$\psi_{ch,fuel} + \left(a + \frac{b}{4}\right) \psi_{ch,O_2} = W_{sh,max} + a\psi_{ch,CO_2} + \frac{b}{2} \psi_{H_2O} \ldots (2.36)$$

As shown earlier,

$W_{sh,max} = -\Delta G_r$ and $\psi_{ch,i} = -RT \ln(x_{io})$

$$\psi_{ch,fuel} = -\Delta G_r + RT \ln\left\{\frac{(x_{O_2,o})^{a+b/4}}{(x_{CO_2,o})^{a} (x_{H_2O,o})^{b/2}}\right\} \ldots\ldots\ldots\ldots\ldots\ldots \quad (2.37)$$

2.5 Simulation Software

Simulation is the imitation of the operations of a facility or process, usually via a computer. To study a system, assumptions/approximations are often made, both logical and mathematical about the system. If the model structure is simple enough, analytical methods could be used to obtained exact solutions. But most systems are too complex and so require complex models which are evaluated numerically and data is usually collected to estimate model characteristics. Such systems must be studied via simulation.

Several computer software have been developed for modelling and simulation of energy systems. Commonly used are Aspen Plus, Aspen Hysys and MATLAB Simulink. With these simulation packages it is possible to model and simulate system in order to predict the behaviour of the system by using engineering relationships such as mass and energy balances, and phase and chemical equilibrium. Given reliable thermodynamic data, realistic operating conditions and rigorous models, actual plant behaviour can be simulated. In the present work, Thermolib software – a tool box which provides sets of thermodynamic model blocks was added to the Simulink library to carry out the simulation. This software was chosen for this work because of the presence of the fuel cell stack model block in its model library. Other software do not and this will require the use of a similar unit in place of the stack which may not give the correct results or modelling the stack unit from the scratch as a user defined unit which is outside the scope of this work.

2.5.1 Thermolib software

Thermolib is a toolbox for MATLAB/Simulink designed for modelling and simulation of energy systems. The toolbox provides a Simulink blockset for system simulations and a set of MATLAB command line functions for thermodynamic calculations and thermodynamic balancing of the simulated models. Thermolib also provides an extendable thermophysical properties database. The blockset includes Simulink blocks for components such as pumps, compressors, valves, heat exchangers, tanks, chemical reactors, fuel cell stacks, burners, etc. All component models focused on the input/output behaviour. The goal is to provide engineers (especially control engineers) with a toolset that enables them to focus on modeling thermodynamic process at the system level, while Thermolib handles the underlying thermodynamics and reaction chemistry (Thermolib – Getting Started, 2013).

The graphical Simulink environment allows for an intuitive design of thermodynamic system models in that the physical flow (usually) follows the signal flow so that model components taken from the library can be arranged in resemblance to the underlying physical topology. While Simulink provides the graphical interface and modeling environment, Thermolib takes care of the special thermodynamic requirements. The user only needs to drag and drop the readymade thermodynamic blocks or process components into his Simulink model. This is much faster than deriving the equation system from the physical conservation laws and integrating them with standard Simulink blocks. Apart from the sheer complexity this task will usually bring about, the above mentioned advantage of graphical programming is lost. Another advantage, perhaps less apparent but even more important is the consistent and very efficient treatment of thermodynamic considerations in the Simulink framework, e.g. fluid mixture properties, state changes involving simultaneous reaction and heat transfer, chemical and phase equilibrium calculations etc.

2.6 Related Works

Frangopoulos and Nakos (2006) noted that fuel cells had not been installed on surface ships yet, but the interest for this type of applications was increasing. In their work, a PEM fuel cell system was studied, that can meet the electric load of a 6500DWT reefer ship. A diesel engine was being used for propulsion of the ship. A thorough thermodynamic and economic analysis was performed and optimization techniques were applied, in order to determine the optimal design and operation mode of the system. Using published information, it was possible to develop an economic model of the system. It was also found that the unit cost of produced electricity was higher than the unit cost of electricity produced by a marine Diesel generator, but the difference was expected to decrease significantly by (i) development of high efficiency

– low platinum electrodes, (ii) decrease in the capital cost of fuel cell units as a consequence of mass production, and (iii) decrease in the price of hydrogen after an increase in production volume.

Yilanci *et al*. (2007) conducted a thermodynamic analysis, in terms of energy and exergy, of a 1.2 kW Nexa PEM fuel cell system in order to investigate its performance in terms of energy and exergy efficiencies at different operating conditions. The results showed that the PEM fuel cell system has high irreversibilities (exergy destructions) resulting in lesser exergy efficiencies compared to the corresponding energy efficiencies.

Obara and Tanno (2008) investigated the exergy flow and exergy efficiency of a 3kW PEM fuel cell, and considered the regional characteristic of the distributed energy system. They noted that when introducing a distributed energy system, consideration of regional characteristics is required. However, no cases of examination using exergy in relation to the regional characteristics of a distributed energy system had been found. It was found that when the same energy system was introduced into a community where climates differ, the exergy flow was shown to vary. The exergy efficiency when the proposed system was introduced into individual houses in Sapporo, Tokyo, and Kagoshima was evaluated. In the case of a load factor of 4 − 100% and an environmental temperature of 263 − 313K, the difference in the total energy efficiency was 6%. On the other hand, the difference in the total exergy efficiency within the same range is 30%. The following methods were suggested for improving exergy efficiency:

a) Preheat the city-gas and air supplied to the system using exhaust heat and raise the combustion temperature.
b) Preheat the water supplied to the system using exhaust heat.

c) In order to reduce the cooling of the reformed gas as much as possible, modify the catalyst material of each unit.

d) Examine the combined cycle power generation.

When the proposed system is introduced into a community with a low outside air temperature, exergy efficiency will increase compared with a community with a high outside air temperature. Moreover, exhaust heat must be released into communities with a high outside air temperature, meaning a considerable drop in energy and exergy efficiencies. On the other hand, because the space cooling load of the system introduced into this community increases; the generation efficiency does the same.

Mukhtar *et al*. (2010) noted that there are numerous design and operating variables that affect the overall performance of a PEM fuel cell system, and that many optimization techniques for the PEM fuel cell system have been reported in the literature. However, most of the reported works considered either efficiency or cost as the objective function. But it has been known that fuel cell efficiency and cost affect each other. Thus, it was imperative to consider both efficiency and cost in order to achieve optimal PEM fuel cell system design. In the paper, a multi-objective function problem to optimize the efficiency and cost of a PEM fuel cell system was formulated. The operating variables considered were: stack temperature, current density, system pressure as well as hydrogen and air flow rates. Many optimum solutions exist for this kind of problem. It was found that one of the optimum solutions was to operate at stack temperature of 353K, system pressure of 0.12MPa, current density of 0.8A/cm^2, hydrogen flow rate of 0.1g/s and air flow rate of 3g/s to produce 5.76kW, at a cost of 522 US $/kW and an efficiency of 52.21%.

San Martin *et al*. (2014) noted that, currently, there is a reduced number of publications that provide experimental data about the performance of fuel cells when

used for supplying Alternating Current (AC). Most of the existing publications provide experimental data only with direct current (DC) loads, or analyze the performance with AC loads using simulation models. For this reason, experimental analysis of the behavior of PEM fuel cell system when feeding different electrical loads was carried out. The results obtained showed a maximum efficiency of 53.2% for a capacity of 153.2W and an efficiency of 41.7% for the rated capacity (1.2kW).

CHAPTER THREE

METHODOLOGY

3.1 Modelling and Simulation of Selected PEM Fuel Cell System Configurations

Five different hydrogen fuel cell system configurations were selected from the literature for detailed study. The selection was based on the systems that use pure hydrogen and can be modeled with Thermolib software. The selected system configurations were tagged as: System 1, System 2, System 3, System 4 and System 5. These are shown in Figures: 3.1 to 3.5. Figure 3.6 shows the proposed system configuration proposed in section 3.3.

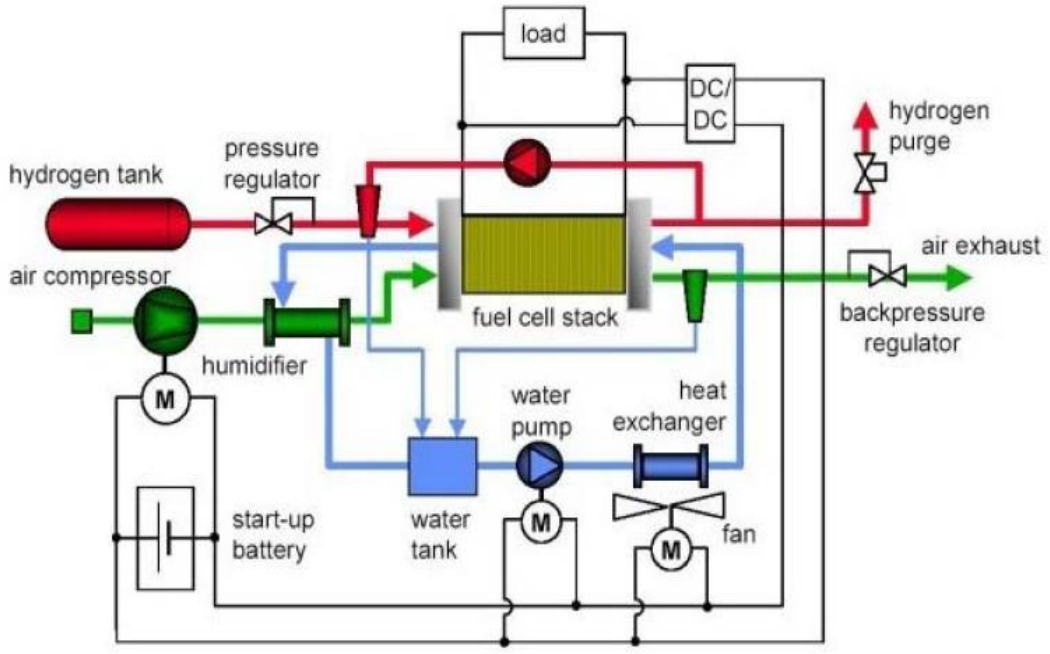


Figure 3.1: System 1 (PEMFCS with air humidification only)
Source: Barbir (2005)

System 1 as shown in Figure 3.1 is composed of the following major equipment: The stack, air compressor, hydrogen blower, air humidifier, cooling water pump and heat exchanger. Pure hydrogen from the storage cylinder mixes with the recycled stream and goes into the stack. The stack also receives a supply of air through the compressor

and humidifier. Cooling water from the water tank is pumped through the heat exchanger into the stack and back through the humidifier.

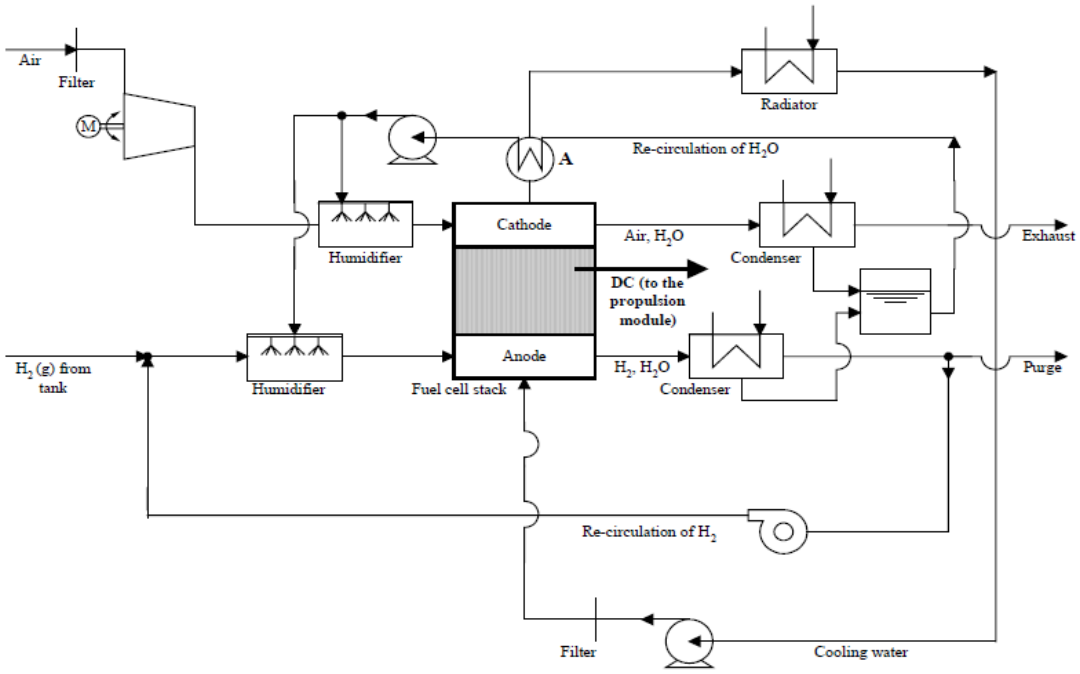


Figure 3.2: System 2 (PEMFCS with anode and cathode exit condensers)
Source: Gurski (2002)

System 2 shown in Figure 3.2 is composed of the stack, air compressor, air and hydrogen humidifiers, pre – heater, hydrogen blower, two condensers, two pumps and radiator. Hydrogen from cylinder (not shown) enters the stack through the humidifier. The exit stream goes into the condenser. Air also goes into the stack through the compressor and humidifier. The exit air also goes into the second condenser. The condensate from both condensers is used to humidify both the air and hydrogen streams. The hydrogen is recycled through the blower. Cooling water is pumped into the stack, pre-heater, radiator and back again.

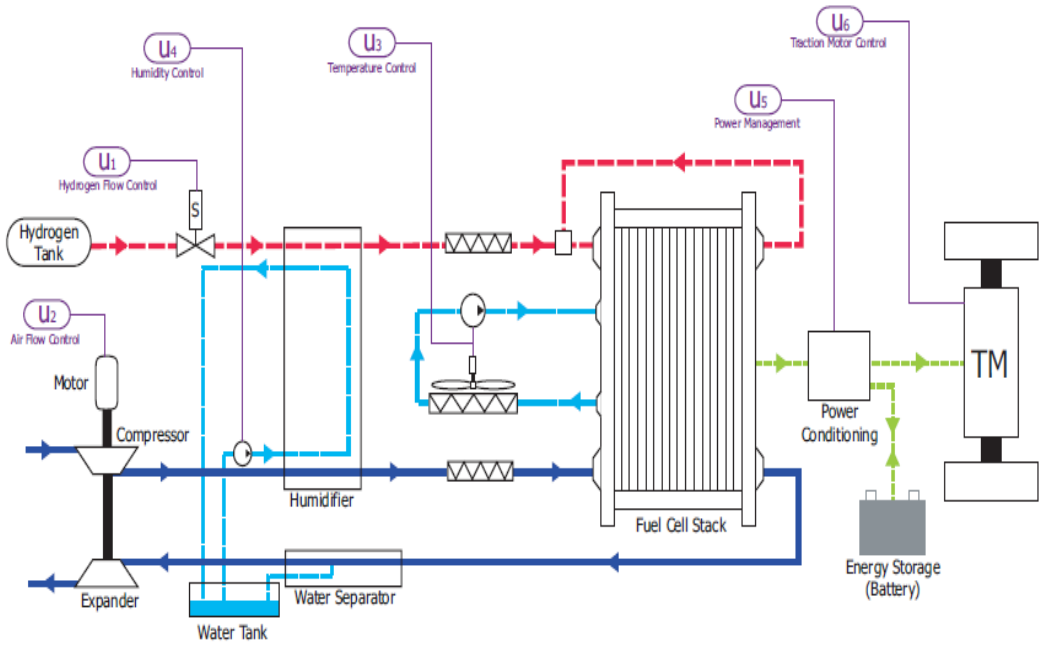


Figure 3.3: System 3 (PEMFCS with anode and cathode pre – heaters)
Source: Pukrushpan *et al*. (2003)

System 3 shown in Figure 3.3 is composed of the stack, the compressor expander module, air and hydrogen humidifiers, air and hydrogen pre-heaters, cooling water pump and radiator. Hydrogen from the tank goes into the stack through the humidifier and pre – heater. The exit stream is recycled. The stack also receives air through the compressor, air humidifier and pre – heater. The exit stream goes out through a water separator and expander.

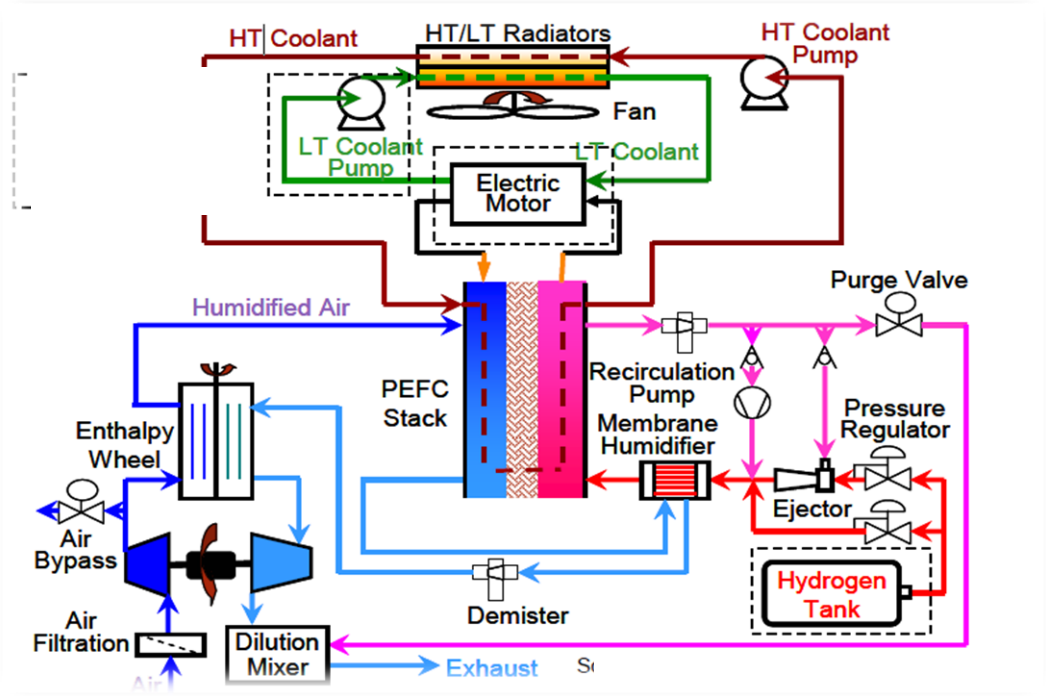


Figure 3.4: System 4 (PEMFCS with enthalpy wheel and membrane humidifiers)
Source: Carlson *et al.* (2005)

System 4 shown in Figure 3.4 is composed of the stack, the compressor expander module (CEM), air humidifier (Enthalpy Wheel), membrane humidifier, hydrogen ejector, hydrogen blower, coolant pump and radiator. Hydrogen from tank goes into the stack through ejector and the membrane humidifier. The exit is recycled through the recirculation blower and ejector. Air goes into the stack through the compressor and air humidifier. The exit air goes into the membrane humidifier, Enthalpy wheel, expander and out through the dilution mixer.

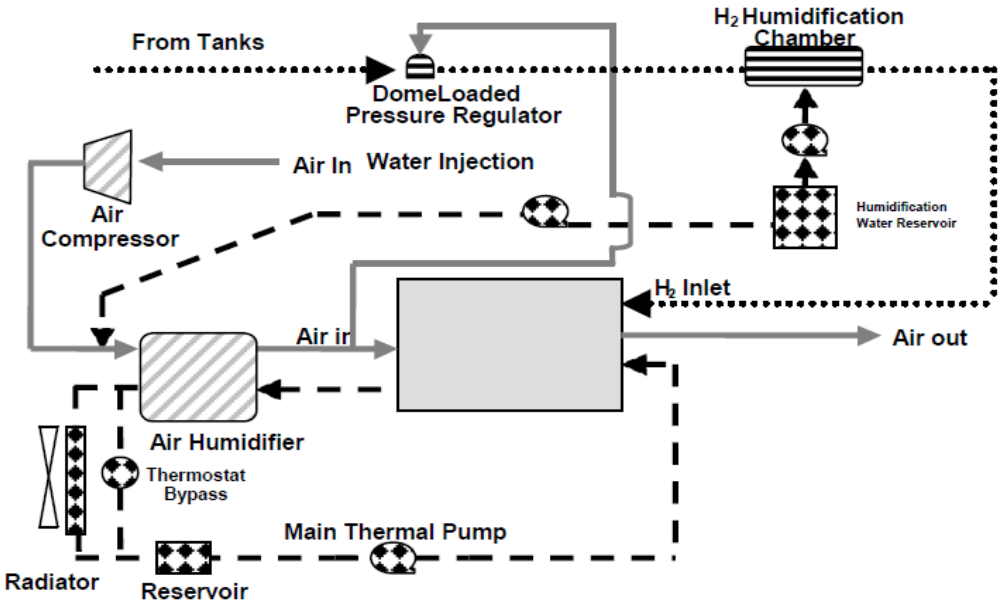


Figure 3.5: System 5 (PEMFCS with separate water source)
Source: Haraldson and Wipke (2004)

System 5 shown in Figure 3.5 is composed of the stack, air compressor, air and hydrogen humidifiers, two humidification pumps, coolant pump and radiator. Hydrogen from tank (not shown) goes into the stack through the humidifier. Air also goes into the stack through the compressor and air humidifier and exits out from the stack. Cooling water is pumped into the stack from the reservoir tank. The hot exit is passed through the air humidifier and radiator and back into the reservoir tank.

Table 3.1 shows the components and distinct features of each of the selected system configuration.

Table 3.1: Components and distinct features of selected system configurations

System	Major Equipment	Distinct Futures
System 1	1. Stack 2. Air compressor 3. Air humidifier 4. Hydrogen recirculation blower 5. Radiator 6. Cooling water pump	- Air humidification only - Stack cooling water is used for humidification - Hydrogen recirculation with blower
System 2	1. Stack 2. Air compressor 3. Air humidifier 4. Hydrogen humidifier 5. Hydrogen recirculation blower 6. Heat exchanger 7. Radiator 8. Cooling water pump 9. Recirculation water pump 10. Cathode exit gas condenser 11. Anode exit gas condenser	- Recirculation water is used for humidification. - Both air and hydrogen are humidified - Hydrogen recirculation with blower. - Anode and cathode exit stream condensers.
System 3	1. Stack 2. Compressor Expander Module (CEM) 3. Air humidifier 4. Hydrogen humidifier 5. Radiator 6. Cooling water pump 7. Recirculation water pump 8. Cathode inlet gas heater 9. Anode inlet gas heater 10. Water separator	- Recirculation water is used for humidification. - Compressor Expander Module (CEM) used for air compression. - Two heaters used to heat anode and cathode inlet streams. - Hydrogen recirculation without blower
System 4	1. Stack 2. Compressor Expander Module (CEM) 3. Air humidifier 4. Hydrogen humidifier 5. Hydrogen recirculation blower 6. Radiator 7. Cooling water pump	- Compressor Expander Module (CEM) used for air compression - Hydrogen recirculation with blower - Both air and hydrogen are humidified. - Enthalpy wheel and membrane types of humidifiers.
System 5	1. Stack 2. Air compressor 3. Air humidifier 4. Hydrogen humidifier 5. Radiator 6. Cooling water pump 7. Two humidification water pump	- Both air and hydrogen are humidified - No hydrogen recirculation - Separate humidification water reservoir

The purpose of the simulation is to obtain data such as operating temperatures, pressures, enthalpies, entropies, molar flow rates, molar fractions of components in each stream, etc in order to carry out the exergy analysis. As mentioned earlier, the system configurations were modelled and simulated using Thermolib software. The software is a product of EUtech Scientific Engineering – a company in Germany (www.thermolib.de). Six months free usage of the software was graciously given by the company for the purpose of this work. For details on how to use this software, refer to (Thermolib – Getting Started, 2013) available from the company's website.

Thermolib models were built by dragging the model blocks such as pumps, compressors, tanks, stacks, etc from the components block of the Thermolib library onto the graphical Simulink environment. These blocks were then interconnected by the streams. The chemical components such as hydrogen, air and water were preset in the model setup block. The default settings in the stack block such as number of cells, hydrogen conversion rate, active membrane area, and reference environment temperature were adjusted by double clicking on a stack block which displayed a dialog box where the specified data were entered. The efficiencies of the compressors and pumps were also specified using the same procedure. Table 3.1 shows the specified system components data based on which the simulations were carried out. These data were selected from the literature (Olgun *et al*., 2004; Obara and Tano, 2006; Yilanci *et al*., 2007; Mukhtar *et al.,* 2010).

Table 3.2: Specified system components data for simulation

Component	Parameter	Value
Stack	Power (kW)	5.00
	Number of cells	40
	Maximum hydrogen conversion rate	0.8
	Total active membrane area (m^2)	0.25
	Reference environment temp. (°C)	25
	Operating temperature(°C)	80
	Operating pressure (bar)	1.5
Compressor	Efficiency (%)	70
Pump	Efficiency (%)	80

The simulation was then run by clicking on the start simulation icon. Provided there are no errors, the simulation will run to completion but if there are any errors, it will stop and prompt the user for necessary adjustments. When the simulation has finished the stream properties such as temperatures, pressures, molar flow rates, enthalpies, etc were read from the display blocks attached to each stream as shown in Figure 3.6. This was done for the five system configurations as well as the proposed system configuration.

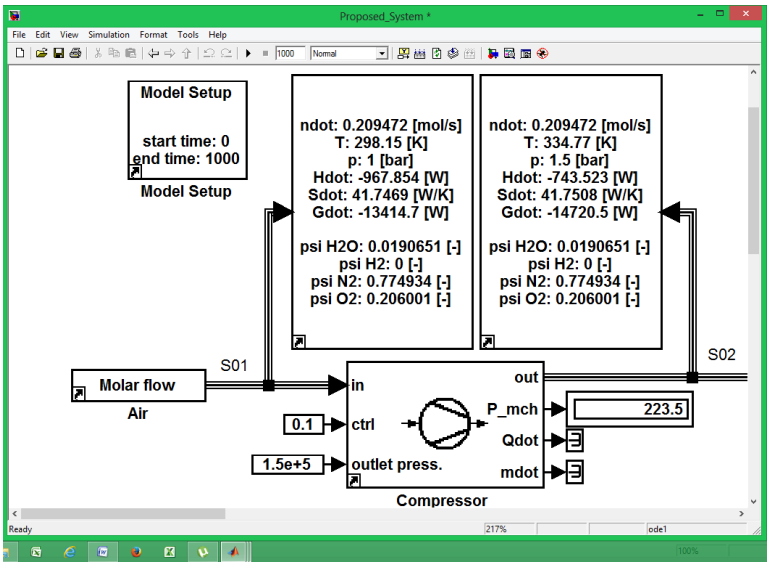


Figure 3.6: Zoomed section showing stream properties

3.2 Exergy Analysis

An exergy analysis was carried out in order to investigate the performances of the different PEM fuel cell system configurations in terms of energy utilization. The results of the simulations were used to carry out the exergy analysis. This was done by calculating the exergy content (Ex_i) of each stream using the following relations (Yilanci *et al.*, 2007):

$$Ex_i = f_i \psi_i \quad \text{(3.1)}$$

$$\psi_i = \psi_{ph,i} + \psi_{ch,i} \quad \text{(3.2)}$$

$$\psi_{ph,i} = (h_i - h_{o,i}) - T_o(s_i - s_{o,i}) \quad \text{(3.3)}$$

$$\psi_{ch,i} = \sum x_{k,i}\, \psi^{o}_{ch,k,i} + RT_o \sum x_{k,i} \ln x_{k,i} \quad \text{(3.4)}$$

where f_i = total molar flow of stream i

$x_{k,i}$ = mole fraction of component k, in stream i

ψ_i = total specific exergy of stream i

$\psi_{ph,i}$ = specific physical exergy of stream i

$\psi_{ch,i}$ = specific chemical exergy of stream i

$\psi^{o}_{ch,k,i}$ = standardspecific chemical exergy of component k in stream i

$h_{o,i}$ = specific enthalpy of stream i at reference conditions

h_i = specific enthalpy of stream i at operating conditions

$s_{o,i}$ = specific entropy of stream i at reference conditions

s_i = specific entropy of stream i at operating conditions

R = the gas constant.

3.2.1 Evaluation of irreversibilities

The irreversibility of each system component was determined using the following relations (Casas *et al*., 2010):

The irreversibility of the fuel cell stack is expressed as:

$$I_{Stack} = -P_{Stack} + \left[\left(f_i.\psi_i\right)_{inlet} - \left(f_i.\psi_i\right)_{outlet}\right]_{cathode} + \left[\left(f_i.\psi_i\right)_{inlet} - \left(f_i.\psi_i\right)_{outlet}\right]_{anode} + \left[\left(f_i.\psi_{ph,i}\right)_{inlet} - \left(f_i.\psi_{ph,i}\right)_{outlet}\right]_{cooling} \quad \text{... (3.5)}$$

where P_{Stack} = stack power.

The irreversibilities of other units were determined using Equation 3.6.

$$I_j = \sum\left(f_i.\psi_{ph,i}\right)_{in} - \sum\left(f_i.\psi_{ph,i}\right)_{out} \quad \text{..... (3.6)}$$

where j represents the jth unit.

3.2.2 Overall system exergy and energy efficiency

The overall exergy efficiency of each system is defined as the ratio of the net power delivered and the exergetic potential of the primary fuel (standard exergy of hydrogen). It is expressed as (Casas *et al.*, 2010):

$$\eta_{Exergy} = \frac{\sum_j W_j}{\left(f_{i,in}.\psi_o^{ch}\right)_{hydrogen}} \quad \text{..... (3.7)}$$

where $\sum_j W_j$ is the net power generated by the system.

On the other hand, the energy efficiency (first law) is calculated based on the LHV of the fuel (hydrogen):

$$\eta_{Energy} = \frac{\sum_j W_j}{\left(f_{i,in}.LHV\right)_{hydrogen}} \quad \text{..... (3.8)}$$

3.3 System Proposition

The results obtained from the exergy analysis (section 4.2) indicated that system 1 has the best performance compared to the other systems being studied. It was also noted that its performance could be further improved by replacing the air compressor with the compressor expander module (CEM) although this is more expensive. This would reduce the parasitic power and hence increase the net power and efficiency of the

system by recovering power from expansion of the exit air stream, which is used to offset the electrical power required for air compression. It was also observed that the hydrogen blower in the hydrogen recirculation line could be removed since the pressure drop across the stack was observed to be insignificant. This would reduce the capital cost of the system. Based on these modifications on system 1, the new system configuration which was expected to be an improved system configuration in terms of energy utilization and cost was proposed. This was also modelled, simulated and analyzed.

3.4 Economic Analysis

The capital cost of each system was estimated by using relations and costs of similar equipment obtained from the literature. The economic indicators – return on investment (ROI) and payback period (PBP) were evaluated and used to compare the economic performances of the systems being studied.

3.4.1 Cost estimation

The capital cost of a complete system was calculated using Equation 3.9.

$$C_{syst} = C_{stack} + C_{anci} \quad \text{(3.9)}$$

where C_{syst} = Capital cost of complete system

C_{stack} = Estimated cost of fuel cell stack

C_{anci} = Estimated cost of ancillary components

The capital cost of the fuel cell stack was estimated using Equation 3.10 (Frangopoulos and Nakos, 2006):

$$C_{Stack} = M\left[\left(\frac{C_1 - 105.4}{10} + \frac{L_p C_p}{21.64}\right)\frac{P_{Stack}(1+d)^N}{P_d} + c_2\right] \quad \text{(3.10)}$$

where M = fixed cost markup (1.1 default)

c_1 = cost parameter ($/m^2)

L_p = fuel cell platinum loading for both electrodes (mg/cm^2)

c_p = platinum cost ($/troy ounce)

P_{Stack} = fuel cell stack power (kW)

P_d = fuel cell power density (W/cm^2)

d = annual fuel cell degradation (%/year)

N = assumed fuel cell useful lifetime (years)

c_2 = stack fixed cost parameter ($).

The fuel cell stack cost depends on the two cost parameters c_1 and c_2 which have been developed for five different production volumes as summarized in Table 3.3. The parameter, c_1 is the power – dependent term (specified in terms of dollar per square metre of membrane area), and the parameter, c_2 is the fixed cost for the fuel cell stack. A production volume of 10,000 units per year was assumed because it represents a moderate value.

Table 3.3: Capital cost parameters for the fuel cell stack

Production Volume (units/year)	**c_1($/m^2$)**	**c_2($)**
100	811.77	1311.30
1,000	722.54	363.33
10,000	454.45	428.51
30,000	329.24	405.79
60,000	312.26	160.98

Source: (Frangopoulos and Nakos, 2006).

Table 3.4 shows the values of economic parameters used for estimation of the costs of the fuel cell stack.

Table 3.4: Values of economic parameters

Parameter	Value
M	1.1
c_1 ($/m^2)	454.45
c_2 ($)	428.51
c_s ($/kg)	5.244
c_p ($/troy ounce)	1100
L_p(mg/cm^2)	0.25
P_d (W/cm^2)	0.5
d (%/year)	6.5
N (years)	15

Extracted from Frangopoulos and Nakos (2006)

The costs of ancillary components were estimated from the costs of similar equipment reported by Direct Technologies, Inc. (DTI) and TIAX in 2009 shown in Table 3.5. The 2009 costs estimates were scaled up for time to obtain the 2014 estimates used in this work, using Equation 3.11:

$$C_2 = C_1 \left(\frac{I_2}{I_1}\right) \quad \text{..... (3.11)}$$

where C_1 = purchase cost in 2009

C_2 = purchase cost in 2014

I_1 = 521.9 (Chemical Engineering Plant Cost Index in 2009)

I_2 = 688.262 (Chemical Engineering Plant Cost Index in 2014)

The Chemical engineering Plant Cost Indexes – I_1 and I_2 were generated using ProEcon – a tool for process economic analysis developed by Dr. S.M. Waziri and H.A. Abubakar of the department of Chemical Engineering, Ahmadu Bello University Zaria – Nigeria.

Table 3.5: Costs estimates in 2009 and 2014

Components	2009 Estimates ($)	2014 Estimates ($)
Compressor	146.3	160.63
Compressor Expander Module (CEM)	327.25	431.56
Membrane Humidifier (for air)	111.00	146.38
Membrane Humidifier (for hydrogen)	59.00	77.81
Direct Water Injected Humidifier	87.93	115.96
Humidifier (EWH)	66.44	87.62
Hydrogen Ejector	42.60	56.18
Hydrogen Blower	222.46	293.37
Condenser reservoir	194.84	256.95
Pressure Regulator	30.95	40.82
Hydrogen Demister	61.00	80.44
Air Demister	156.00	205.73
Air/Hydrogen Mixer	27.00	35.61
Purge Valve	15.00	19.78
Check Valve	10.00	13.19
Air Filter	4.00	5.28
Air Precooler	43.00	56.71
Radiator	64.68	85.30
Radiator Fan	75.00	98.91
Re-circulation Pump	30.00	39.56
Cooling Pump	63.00	83.08
Control, Wiring, Piping	278.29	367.00

Extracted from Sinha (2010)

3.4.2 Economic indicators

The economic indicators were evaluated based on the following assumptions:

1. Capacity – Annual operation time 6480h/yr.
2. Analysis period – Analysis is carried out for the assumed life cycle costs over a period of 15 years, after which it is assumed that all equipment have zero value and will be replaced.

3. Price of electricity from fuel cell source $0.185/kWh (Adams, 2011)
4. Installation cost is 20% of system purchase price (Adams, 2011).
5. Fuel cell system maintenance cost is 9% of purchase price (Adams, 2011)
6. Hydrogen price is 1.2$/kg (Adams, 2011)

Total capital investment (TCI) = Fixed capital investment (FCI) + Annual operating costs.

Fixed Capital Investment (FCI) = System purchase price + Cost of installation.

= 1.2 x System purchase price.

= 1.2 x (1– 0.3) x System purchase price (including tax credit of 30%).

= 0.84 x System purchase price

Annual fuel cost ($/yr) = System fuel consumption rate (kg/h) x Annual operation time (h/yr) x fuel price ($/kg).

Annual maintenance cost ($/yr) = 9% of System purchase price.

Annual operating costs ($/yr) = Annual fuel cost + Annual maintenance cost.

System annual power output (kWh/yr) = Net power x Annual operation time.

Annual income (Sales) ($/yr) = Annual power output x Unit price.

Annual operating income ($/yr) = Annual income (sales) – Annual operating cost.

Annual depreciation (straight line assuming 15 years useful life time)

Income before tax ($/yr) = Annual operating income – Annual depreciation.

Income after tax (25% tax) = 0.75x Income before tax.

Annual cash income ($/yr) = Income after tax + depreciation

Annual cash flow ($/yr) = Annual cash income + Total capital investment (TCI)

Payback period (PBP) = Fixed capital investment (FCI) ÷ Annual cash income

Return on investment (ROI) = Income after tax ÷ Fixed capital investment (FCI) × 100

CHAPTER FOUR

RESULTS AND DISCUSSIONS OF RESULTS

4.1 Simulation Results

The models of the systems built using Thermolib model blocks are shown in Figures A1 – A6 of Appendix A. Figure 4.1 shows the stack temperature, stack power and current signals displayed by the scope block during the simulation run. It can be seen that the stack temperature rises from 320K to about 385K and is quickly brought down and maintained at about 353K by the action of the controller. The controller controls the stack temperature by adjusting the flow rate of cooling water through the stack from the cooling water pump. The output power and current signals are also observed to rise from zero to 5000W and about 313A respectively. Similar displays were obtained for all systems during simulation.

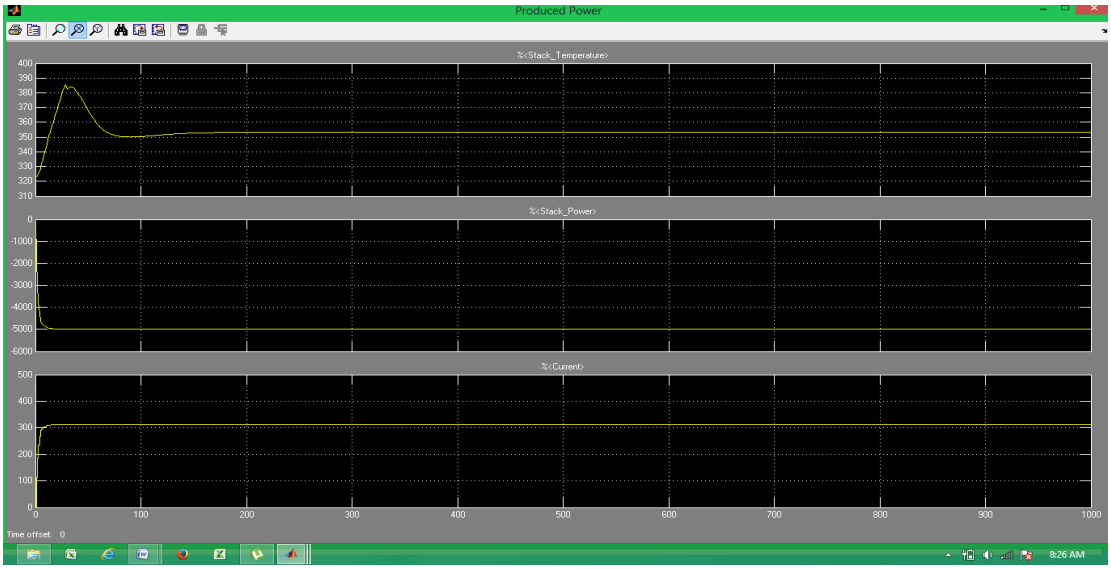


Figure 4.1: Simulation results

The stream properties such as temperatures, molar flow rates, enthalpies, etc read from the display blocks attached to all streams and the calculated exergy contents of each stream are shown in Tables B1 to B6 of Appendix B.

4.2 Exergy Analysis Results

Figure 4.2 shows the irreversibilities (or exergy losses) that occur in each of the components of system 1 and Figure 4.3 shows their exergy efficiencies.

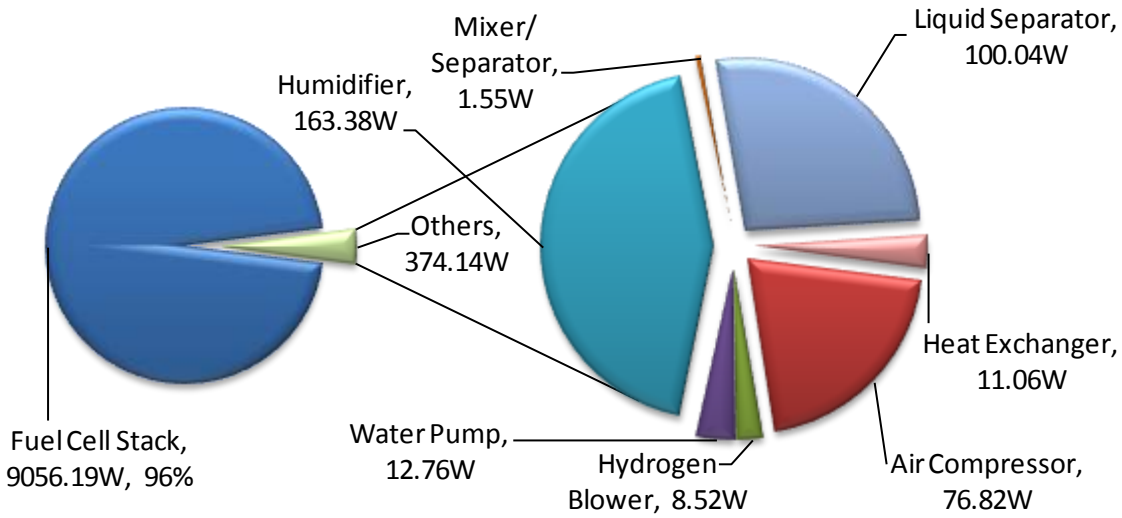


Figure 4.2: Irreversibilities of system 1 components

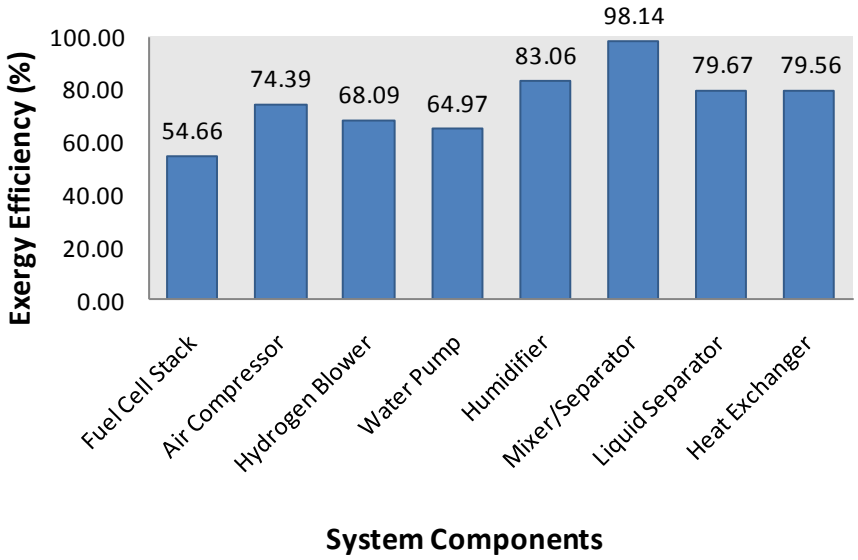


Figure 4.3: Exergy efficiencies of system 1 components

It can be seen from Figure 4.2 that the irreversibility (or exergy loss) that occurs in the fuel cell stack alone is 9059.19W which represents 96% of the total

irreversibility of the system. The total irreversibility (loss contribution) of other units or components of the system is only 374.14W which also represents the remaining 4%. This shows that the fuel cell stack is highly irreversible. This is due to the contribution of the chemical exergy change that occurs as a result of the electrochemical reactions taking place in the fuel cell stack. Other system units do not involve any chemical processes and besides, their operating conditions (temperatures and pressures) are very low which explains their low irreversibilities. Similar results have been reported by Delsman *et al*. (2006) and Casas *et al*. (2010). Figure 4.3 also shows the performance of the individual components of the system in terms of exergy efficiency. Exergy efficiency is defined as the ratio of the exergy output of a system unit to the exergy input to the unit. It can be seen from this figure that the mixer/separator and humidifier perform very well in terms of efficiency, followed by liquid separator and heat exchanger. The fuel cell stack does not perform very well and should be considered when optimizing the system.

Similar results were also obtained for systems 2 to 5 as well as the proposed system configuration as presented in Figures 4.4 to 4.13.

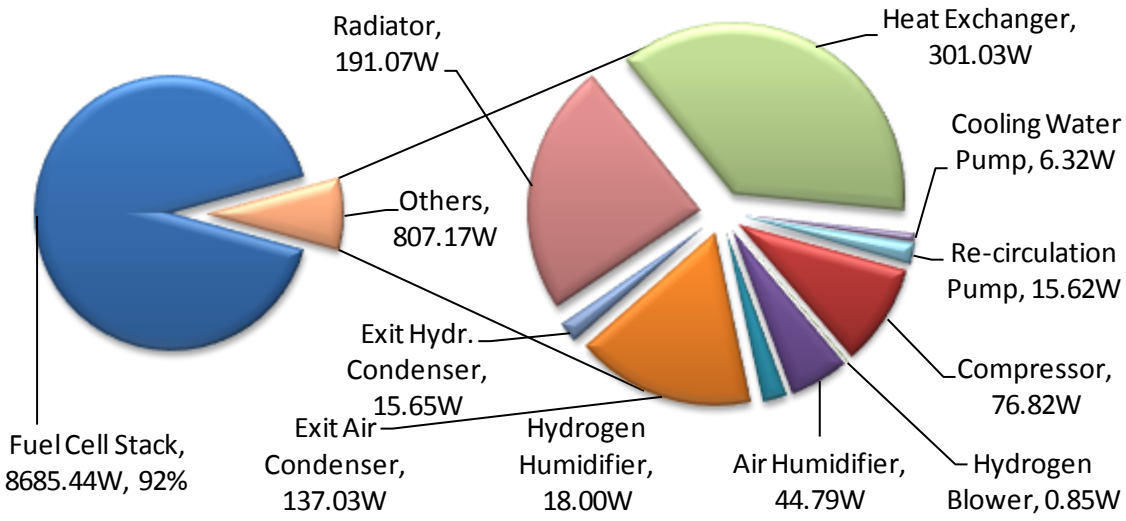


Figure 4.4: Irreversibilities of system 2 components

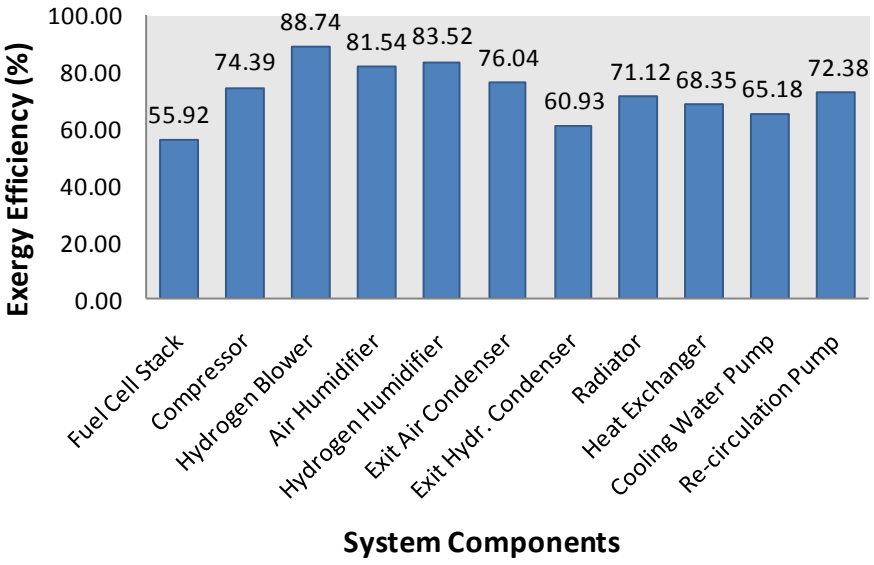


Figure 4.5: Exergy efficiencies of system 2 components

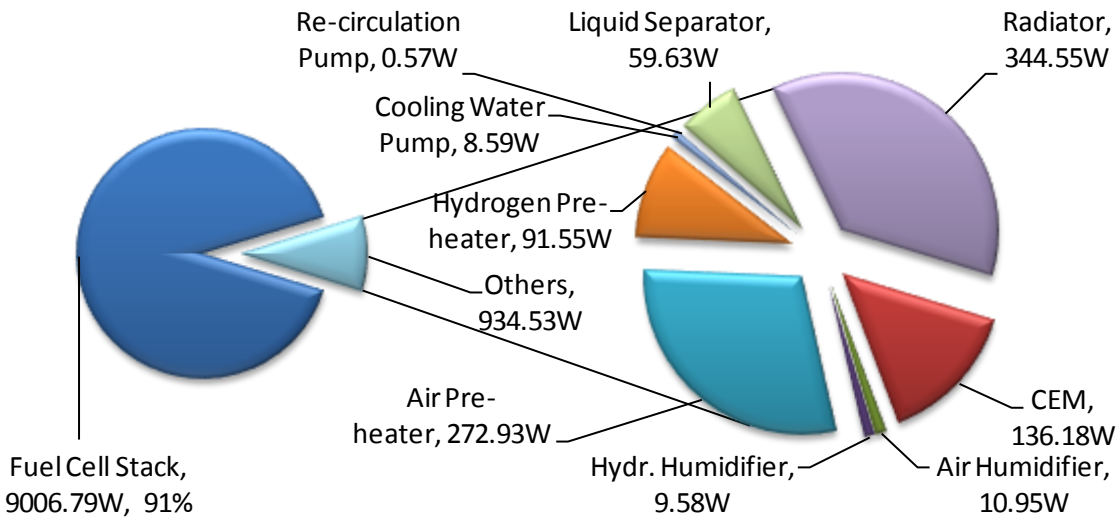


Figure 4.6: Irreversibilities of system 3 components

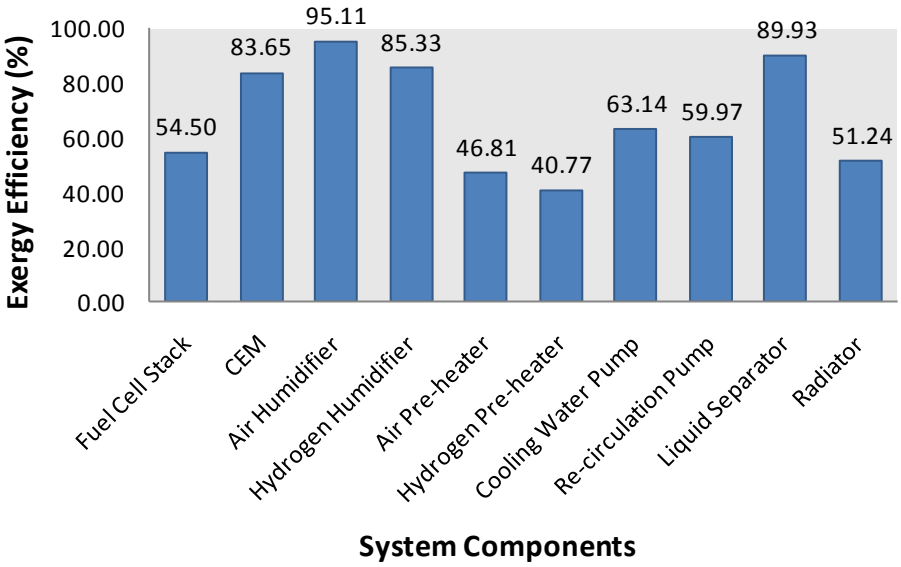


Figure 4.7: Exergy efficiencies of system 3 components

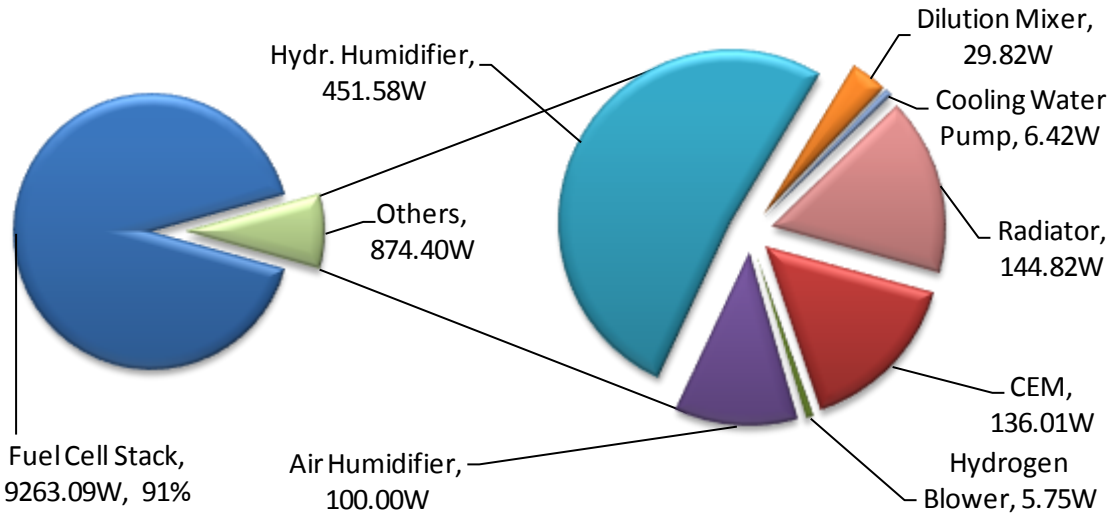


Figure 4.8: Irreversibilities of system 4 components

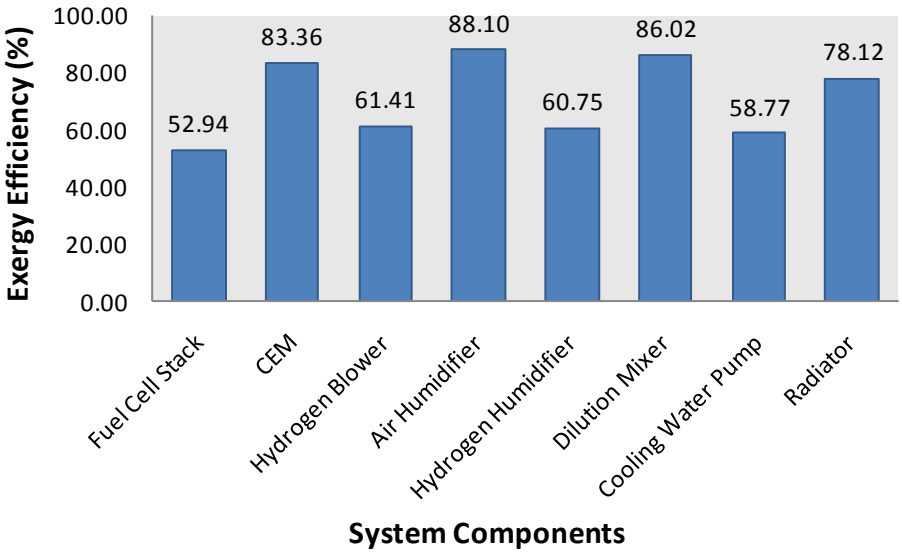


Figure 4.9: Exergy efficiencies of system 4 components

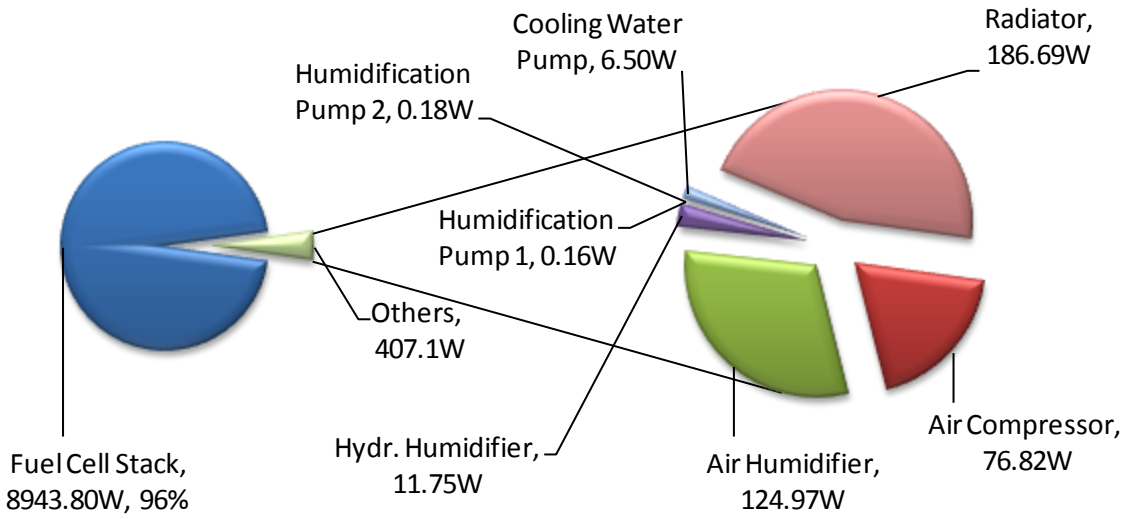


Figure 4.10: Irreversibilties of system 5 components

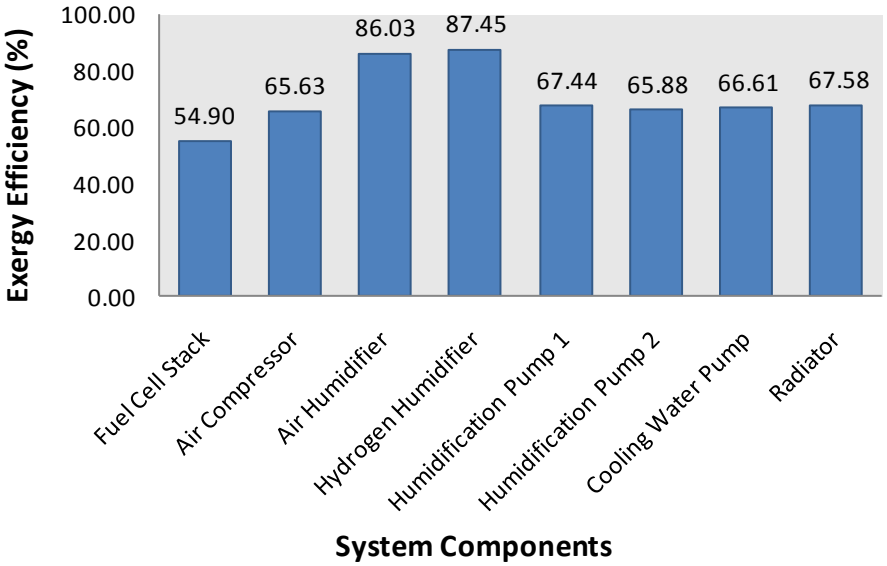


Figure 4.11: Exergy efficiencies of system 5 components

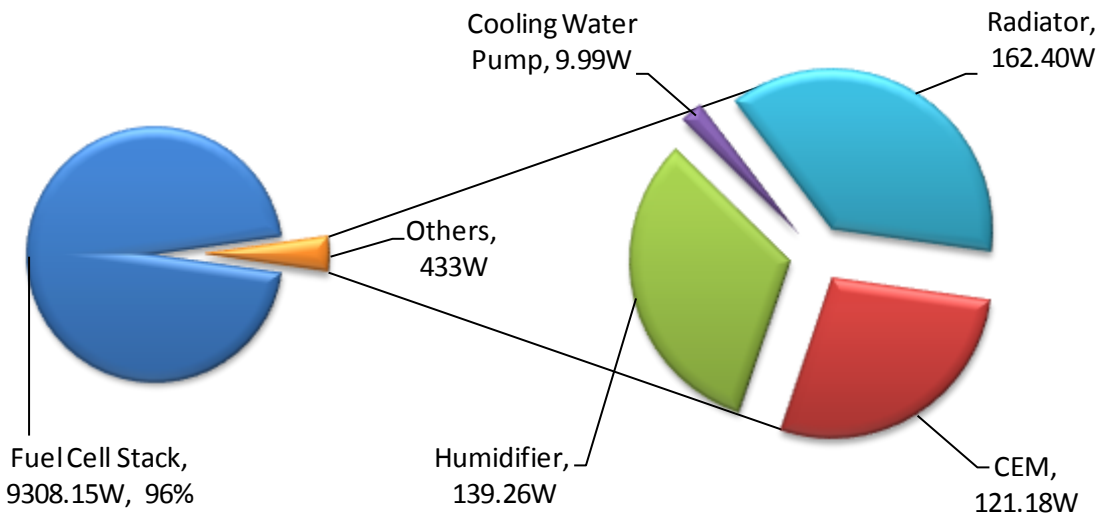


Figure 4.12: Irreversibilities of proposed system components

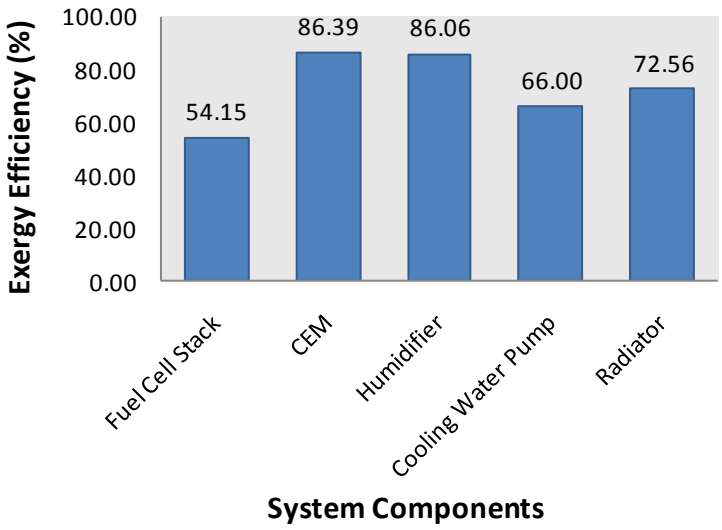


Figure 4.13: Exergy efficiencies of proposed system components

It can be seen from Figures 4.4, 4.6, 4.8, 4.10 and 4.12 for systems 2 to 5 and the proposed system that the largest exergy loss occurs in the fuel cell stack (over 90% of the total losses). Figures 4.5, 4.7, 4.9, 4.11 and 4.13 also show the performance of the components of these systems in terms of exergy efficiency. The exergy efficiency of the fuel cell stack in the respective systems lies between about 52.94% and 55.92%. This

implies that the loss in the stack accounts for about 44 to 47% of the total loss that occur for each system. The exergy efficiencies of some of the other components are up to 95% which is very good.

Figure 4.14 shows the overall exergy and energy efficiencies of systems 1 to 5 as well as the proposed system configuration.

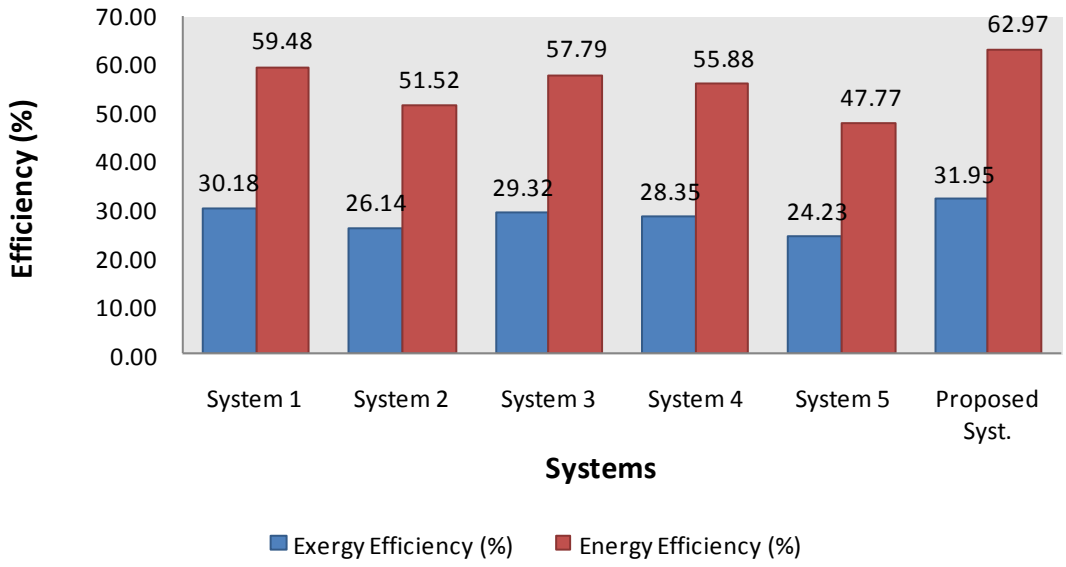


Figure 4.14: Overall exergy and energy efficiencies of each system

The overall exergetic and energetic efficiencies refer to a whole system and are defined by the ratios of the system net power output to the exergetic potential of the fuel (standard exergy of hydrogen) and lower heating value (LHV) of hydrogen, respectively. It can be seen that the overall exergetic efficiencies of systems 1 to 5 as well as the proposed system lie between 24.23% and 31.95% while their energetic (first law) efficiencies lie between 47.77% and 62.97% as shown in Figure 4.14.

Figure 4.15 shows the net power delivered by each system. It can be observed that the proposed system delivered the highest net power followed by system 4. This is because of the presence of the compressor expander module (CEM) in these systems which reduce the power required for air compression. The CEM is also present in

system 3 however; it delivered the least net power. This is because of the presence of the pre – heaters which led to a high parasitic power in the system.

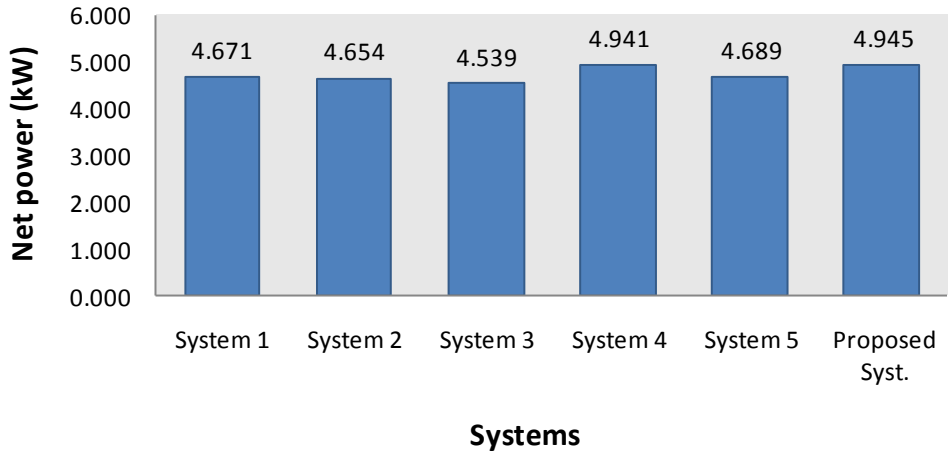


Figure 4.15: Net power produced by each system

Figure 4.16 shows the fuel (hydrogen) consumption rates in kilograms per hour of systems 1 to 5 as well as the proposed system.

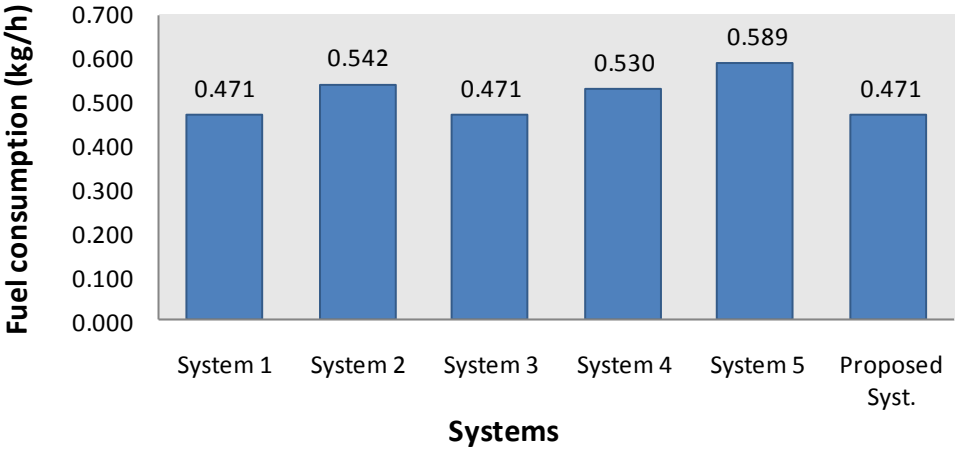


Figure 4.16: Fuel consumption of each system

It can be seen that system 5 consumes the greatest amount of fuel per hour compared to the other systems. This is perhaps due to the absence of hydrogen recirculation. And because of this high fuel consumption rate, system 5 is less efficient as shown in Figure 4.14.

4.3 System Proposition Results

The proposed system configuration shown in Figure 4.17 is composed of the fuel cell stack, the compressor expander module (CEM), the air humidifier, the radiator and the cooling water pump. This system is distinct from others by having a small number of units arranged in the most efficient way. The compressor expander module (CEM) ensures that the power required to compressed air is lower compared to when a compressor unit is used.

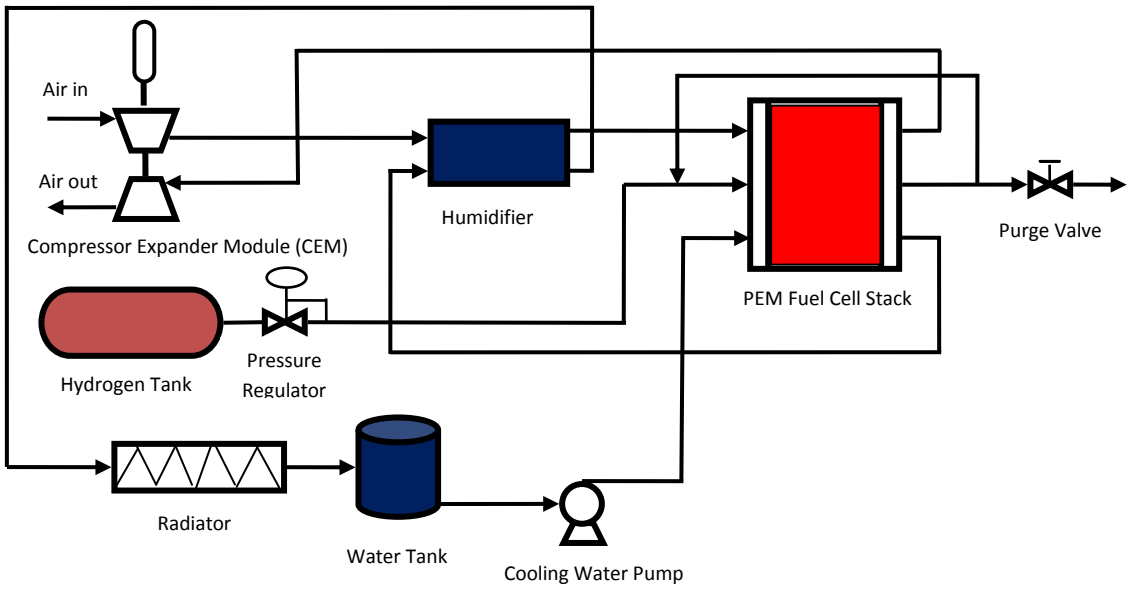


Figure 4.17: Proposed System Configuration

This helps to improve the net power and hence the overall efficiency of the system. The recirculation also ensures good fuel utilization.

4.4 Economic Analysis Results

The economic analysis was carried out by estimating the cost of each system from the cost estimates of its individual components. Figure 4.17 shows the costs estimated for each system while Figure 4.18 shows these cost estimates when expressed per kilowatt of net power for each system.

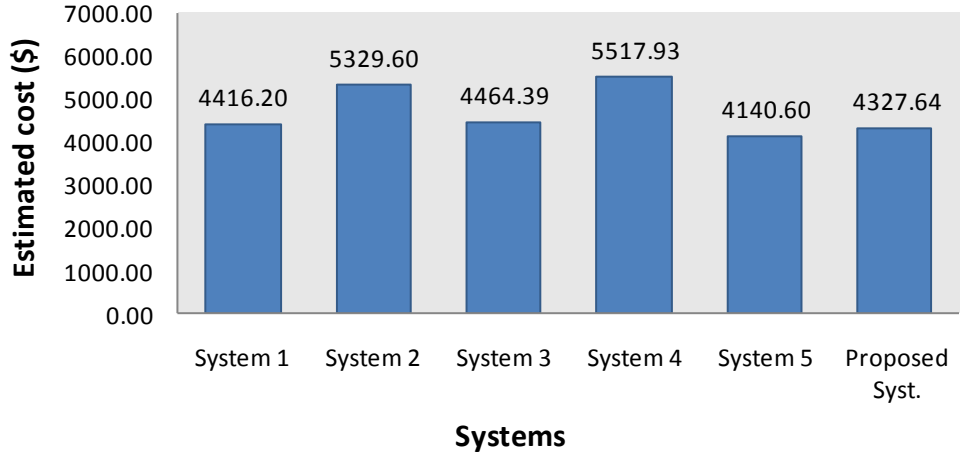


Figure 4.18: Estimated costs of each system

It can be observed from Figure 4.18 that system 4 has the highest cost estimate followed by system 2, system 3, system 1, proposed system and system 5 in that order. When these cost estimates were expressed per kilowatt of net power, the trend was observed to change among systems 1 and 4 and system 5 and the proposed system. This is due to system 4 and the proposed system having higher net power than system 2 and system 5, respectively. The proposed system recorded the least cost of $875.13/kW among the six systems investigated.

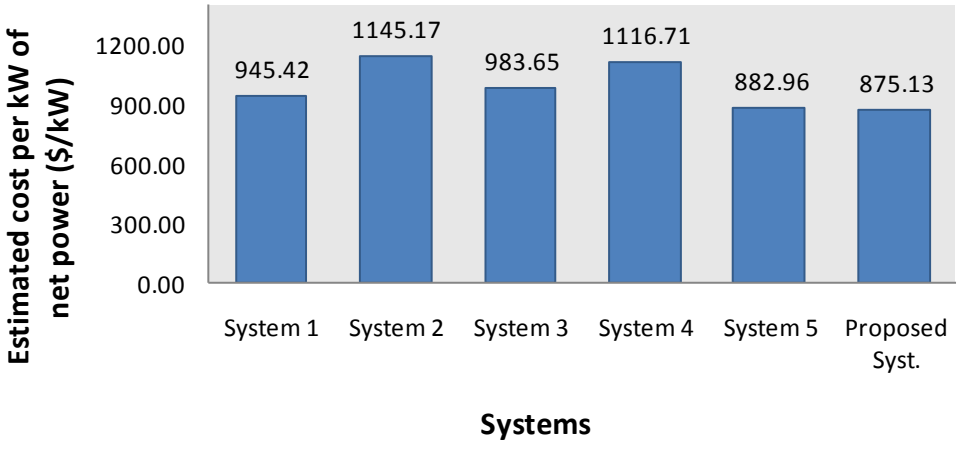


Figure 4.19: Estimated costs of each system based on net power

Figure 4.20 shows the values of the economic indicators – pay-back period and return on investment (evaluated based on the assumptions presented in section 3.4.2) in order to compare the performance of the systems. A lower payback period and a higher return on investment indicate good performance.

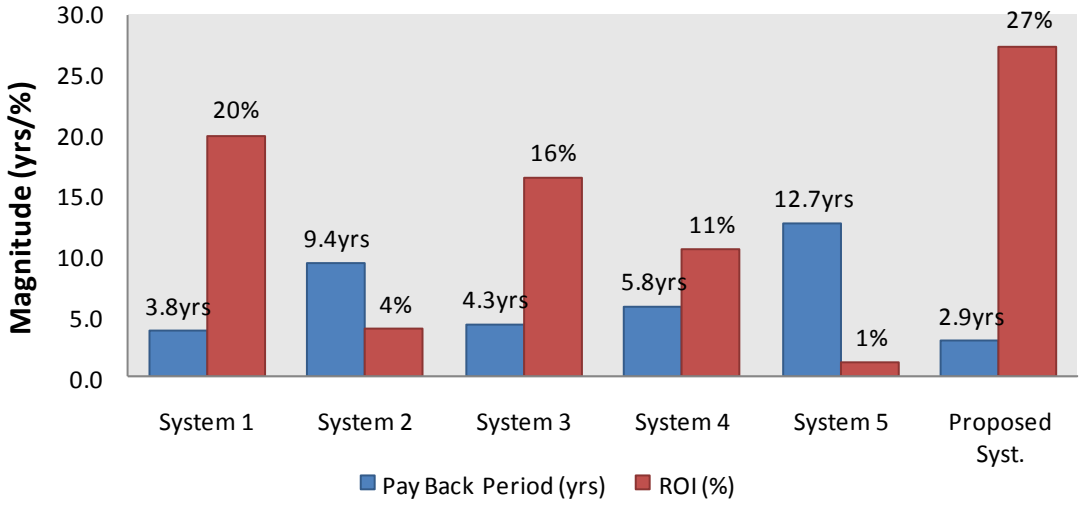


Figure 4.20: Systems economic indicators

It can be seen that the proposed system has the lowest pay – back period of approximately 3 years and the highest ROI of 27%. This is followed by system 1 (about 4 years and 20%), system 3 (about 4 years and 16%), system 4 (about 6 years and 11%), system 2 (about 9 years and 4%) and system 5 (about 13 years and 1%). This indicates the order of economic performance of the systems.

In terms of both energy utilization and cost, the proposed system configuration has the best performance, followed by system 1, system 3, system 4, system 2 and system 5, respectively.

The study has:

1. Compared the performance of five different PEM fuel cell system configurations in terms of energy utilization and cost and established that the overall exergetic

and energetic efficiencies of the systems lie between 24% and 30% and between 48% and 59%, respectively.

2. Developed an improved system configuration that shows an improvement of 1.77% and 3.495% on the overall exergy and energy efficiencies, respectively, on the best of the five different system configurations studied.

CHAPTER FIVE

CONCLUSIONS AND RECOMMENDATIONS

5.1 Conclusions

A study of different PEM fuel cell system configurations that have been reported in literature has been carried out. Five different systems were selected for the detail work. An exergy and economic analysis in order to investigate the performance of the selected systems has also been carried out. Thermolib software was used to model and simulate the different systems in order to obtain the required data for the analysis.

The results indicated that the largest exergy loss occurs in the stack (over 90%) for each of the systems. The overall exergetic and energetic efficiencies of the selected systems lie between 24.23% and 30.18% and between 47.77% and 59.48%, respectively. Among the five systems considered, system 1 showed the highest exergy and energy efficiencies of 30.18% and 59.48%, respectively. This is followed by system 3 (29.32% and 57.79%), system 4 (28.35% and 55.88%), system 2 (26.14% and 51.52%) and system 5 (24.23% and 47.77%). However, an improved system configuration was proposed, modelled and analyzed. Its exergy and energy efficiencies of were found to be 31.95% and 62.97%, respectively. The results of the economic analysis show that the proposed system has the best performance as indicated by its PBP of 2.9 years and ROI of 27%. This is followed by system 1 (3.8 years and 20%), system 3 (4.3 years and 16%), system 4 (5.8 years and 11%), system 2 (9.4 years and 4%) and system 5 (12.7 years and 1%).

This study has therefore, shown that the proposed system configuration has the best performance in terms of both energy utilization and cost. This is followed by system 1, system 3, system 4, system 2 and system 5, respectively.

5.2 Recommendations

Based on this study, the following recommendations were made:

1. Having observed the high performance of the proposed system configuration, a prototype of the proposed system configuration should be fabricated.
2. The department should acquire simulation software packages that would assist students in conducting similar research.
3. A similar study should be carried out on the other types of fuel cell system configurations to identify the most efficient designs.

REFERENCES

Adams, A. (2011). Cost analysis comparison of bloom energy fuel cells with solar energy technology and traditional electric companies (A project report, San Jose State University). Retrieved from http://www.generalengineering.sjsu.edu/docs/pdf/mse_prj_rpts/spring2 (25/05/2014)

Barbir, F. (2005). *PEM Fuel Cells*. Retrieved from http://www.springer.com/cda/content/document/ (21/01/2013)

Barbir, F., Nadal, M. and Fuchs, M. (1999). Fuel Cell Powered Utility Vehicles. *Proc. of the Portable Fuel Cell Conference*in Buchi, F. (editor), pp. 113–126.

Basualdo, M.S., Feroldi, D. andOutbib, R. (2012). PEM Fuel Cells with Bio-Ethanol Processor Systems. *Green Energy and Technology.* doi: 10.1007/978-1-84996-184-4_2

Carlson, E.J., Kopf, P., Sinha, J., Sriramulu, S. and Yang, Y. (2005). *Cost analysis of PEM fuel cell systems for transportation* (Subcontract report NREL/SR-560-39104. Retrieved from http://www.eere.energy.gov/hydrogenandfuelcells/pdfs/tiax_fc_cost_analysis_2005.pdf (21/01/2013)

Casas, Y., Arteaga, L.E., Morales, M., Rosa, E., Peralta, L.M. and Dewulf, J. (2010). Energy and exergy analysis of a methanol fueled solid oxide fuel cell power plant. *Chemical Engineering* Journal, 162(3), 1057 – 1066. doi: 10.1016/j.cej.2010.06.02

Chemical Exergy. (n.d.) [PowerPoint slides]. Retrieved from http://www.oocities.org/pldhar/Lecture7_5.ppt (02/01/2013)

Delsman, E.R., Uju, C.U., de Croon, M.H.J.M., Schouten, J.C., Ptasinski, K.J. (2006). Exergy analysis of an integrated fuel processor and fuel cell (FP–FC) system. *Energy*, 31(15), 3300 –3309. doi:10.1016/j.energy.2006.03.011

Frangopoulos, C.A. and Nakos, L.G. (2006). Development of a model for thermoeconomic design and operation optimization of a PEM fuel cell system. *Energy*, 31(10), 1501–1519. doi: 10.16/j.energy.2005.05.026

Gurski, S. (2002). *Cold Start Effects on Performance and Efficiency for Vehicle Fuel Cell System* (Master of Science Thesis, Virginia Polytechnic Institute and State University). Retrieved from http://www.scholar.lib.vt.edu/theses/available/etd-12192002-162600/u (24/01/2014)

Haraldsson, K. and Wike, K. (2004).Evaluating PEM fuel cell system models. *Journal of Power Sources*, 126(1), 88 – 97. doi: 10.1016/j.jpowsour.2003.08.044

Jafarmadar, S. (2012). The Numerical Analysis of H_2/Air Combustion with Detail Kinetic Simulation Model. *International Journal of Engineering*, 25(3) 239 – 247

Kotas, TJ. (2004). *Theexergy method of thermal plant analysis*. doi: 10.1002/cite.330690828

Lanz, A., Heffel, J. and Messer, C. (2001). *Hydrogen fuel cell engines and related technologies*. Retrieved from http://www.ntl.bts.gov/lib/12000/12200/12207/index.html (25/08/2014)

Mukhtar, B., Zaidi, J.S. and Faqir, N.M. (2010). Multi – Objective Function Optimization for PEM Fuel Cell System. *ECS Transactions*, 26 (1) 77 – 88.doi: 10.1149/1.3428978

Nuhu, M., Olawale, A.S., Salahudeen, N., Yusuf, A.Z., and Mustapha, Y. (2012). Exergy and energy analysis of fluid catalytic cracking unit of Kaduna Refining and Petrochemical Company. *International Journal of Chemical Engineering and Applications,* 3(6), 441 – 445.

Obara, S. and Tanno, I. (2008). Exergy analysis of a regional-distributed PEM fuel cell system. *International Journal of Hydrogen Energy* 33(9), 2300 – 2310. doi: 10.106/j.ijhydene.2008.02.036

Olgu, H., Ersoz, A., Kaya, D., Tiris, M., Akgun, F. and Ozdogan, S. (2004). Simulation Study of a PEM Fuel Cell System with Steam Reforming. *Internation Journal of Green Energy,* 1(3), 313 – 325. doi: 10.1081/GE–200033613

Pukrushpan, J.T. (2003). *Modeling and control of fuel cell systems and fuel processors,* (A dissertation, University of Michigan). Retrieved from http://www.personal.umich.edu/~annastef/FuelCellPdf/pukrushpan_thesis.pdf (10/01/2013)

Rayment, C. and Sherwin, S. (2003). *Introduction to Fuel Cell Technology.* University of Notre Dame. Available from http://www.www3.nd.edu (05/02/2013)

Sanghai, Y.S. (2013). *Techno-economic analysis of hydrogen fuel cell systems used as an electricity storage technology in a wind farm with high amounts of intermittent energy* (Master's dissertation, University of Massachusetts Amherst). University of Mumbai, India. Retrieved fromhttp://www.scholarworks.umass.edu/cgi/viewcont... (19/03/2013)

SanMartín, J.I., Zamora, I., Aperribay, V., SanMartin, J.J., Eguia, P. and Torres, E. (2014). Performance analysis of PEM fuel cells with different electrical loads. *Fuel Cells*, 14(2), 312 – 324.doi: 10.1002/fuce.201300092

Sinha, J. (2010). *Cost analysis of fuel cell stacks/systems*. (FY 2010 Annual progress report). Retrieved from http://www.hydrogendoedev.nrel.gov/pdfs/progress10/v_a_3_sinha.pdf (11/04/2013)

Thermodynamics of Fuel Cells. (n.d.): Lecture notes. Retrieved from http://www.engr.uconn.edu/~jmfent/CHEG320_thermodynamics%20lecturesGrayscale.pdf (22/10/2012)

Thermolib – Getting Started. (2013). Germany: EUtech Scientific Engineering GmbH. Available from www.thermolib.de (01/06/2013)

Thomas, S. andZalbowitz, M. (2000).*Fuel Cells Green Power*. Los Alamos National Laboratory. Retrieved from http://www.lanl.gov/../Green%2520Power.pdf(25/08/2014)

Vosough, A., Noghrehabadi, A., Ghalambaz, M. and Vosough, S. (2011). Exergy Concept and its Characteristic. *International Journal of Multidisciplinary Sciences and Engineering*, 2(4), 2045 – 2057.

Wang, Y., Chen, K., Mishler, J., Cho, S.C. and Adroher, X.C. (2011). A review of polymer electrolyte membrane fuel cells: Technology, applications, and needs on fundamental research. *Applied Energy,* 88(4), 981–1007. doi: 10.1016/j.apenergy.2010.09.030

Yilanci, A., Ozturk, H.K., Atalay, O. and Dincer, I. (2007). Exergy Analysis of a 1.2 kW PEMFC system: *Proceedings of third International Energy, Exergy and Environment Symposium.* University of Ontario Institute of Technology, L1H 7K4,

Canada. Retrieved from http://www.net/profile/Harun_Ozturk/publication/228 (09/01/2013)

Appendix A: Thermolib Models of Systems

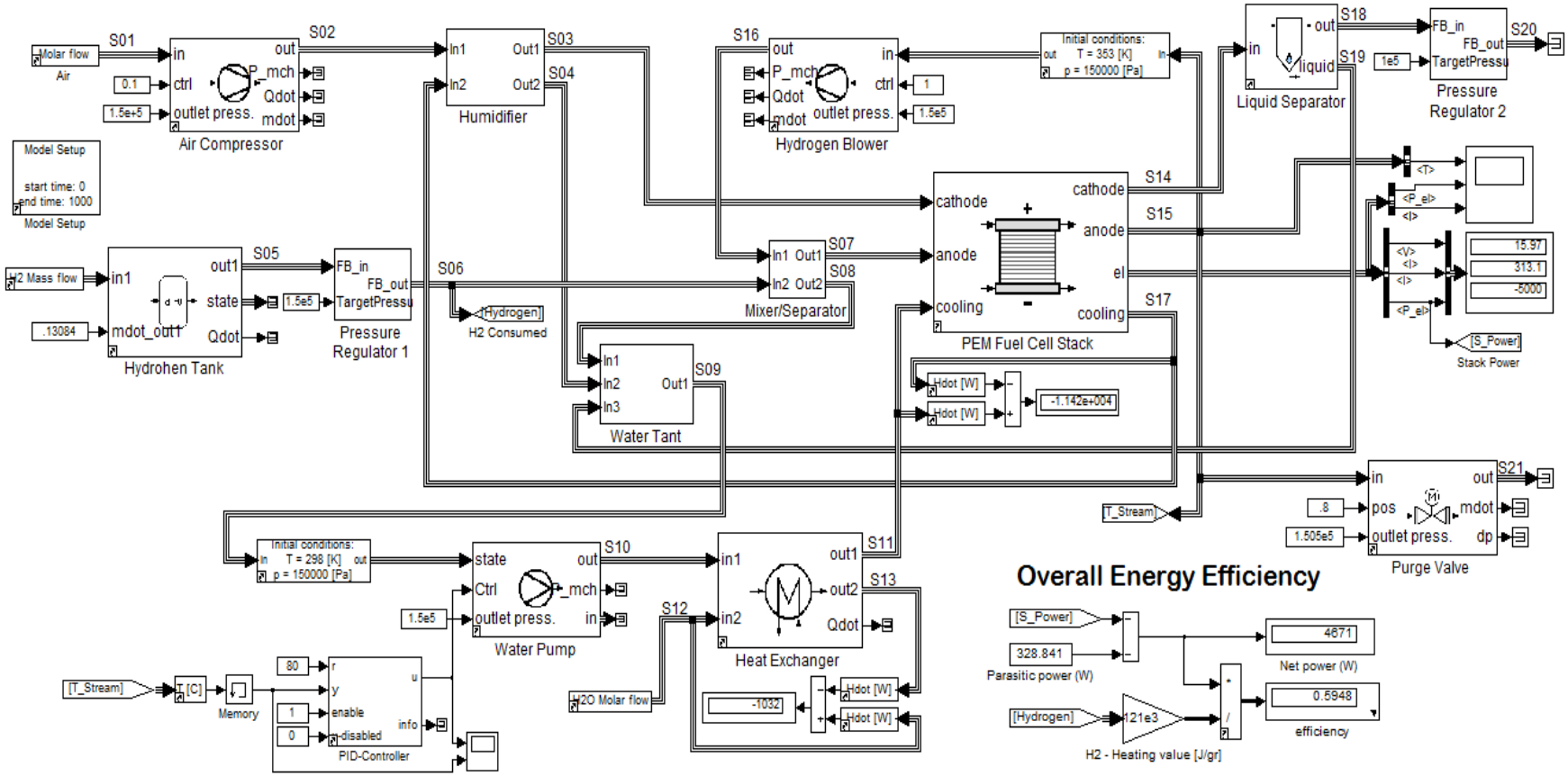


Figure A1: Thermolib model of system 1

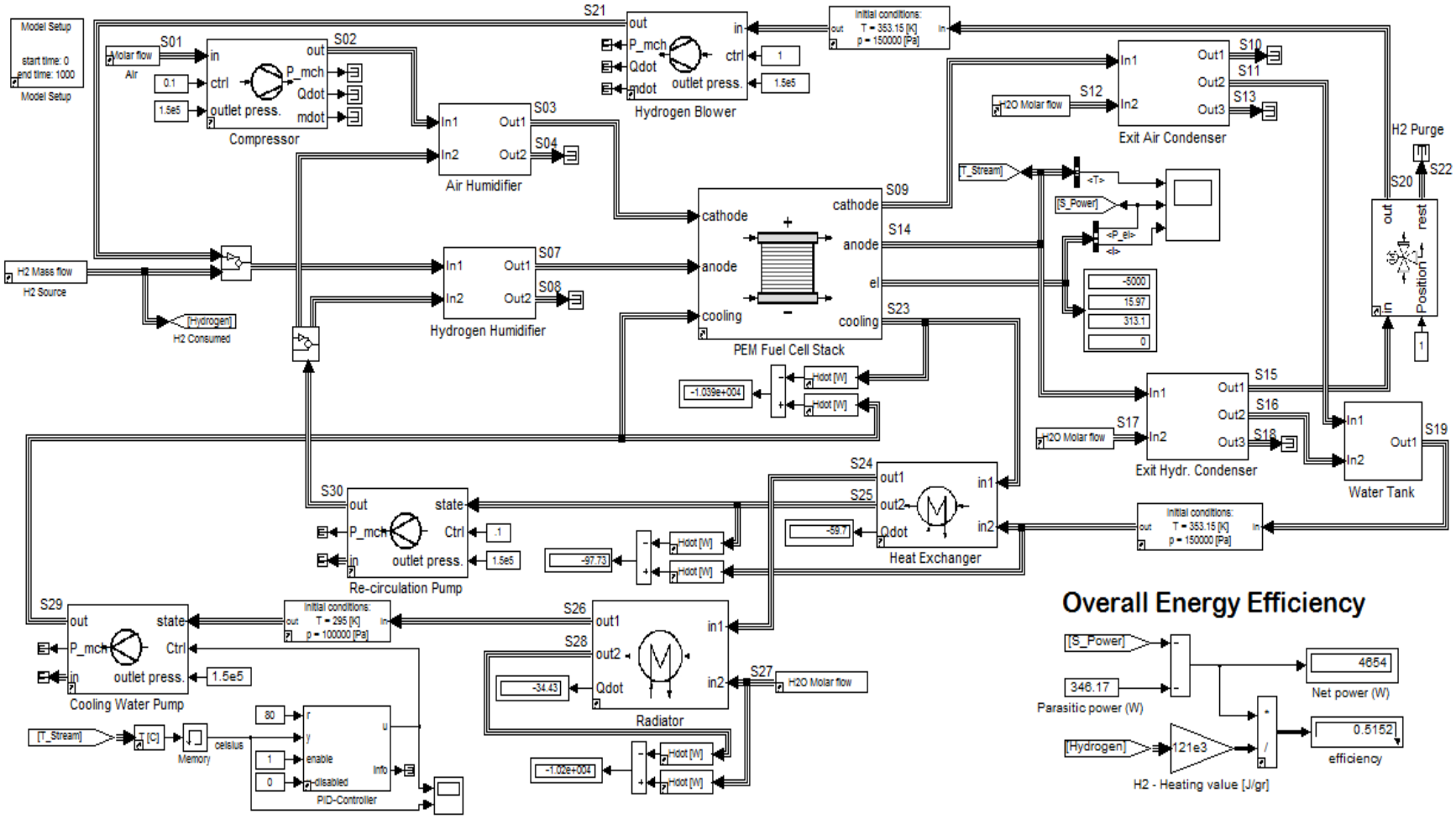


Figure A2: Thermolib model of system 2

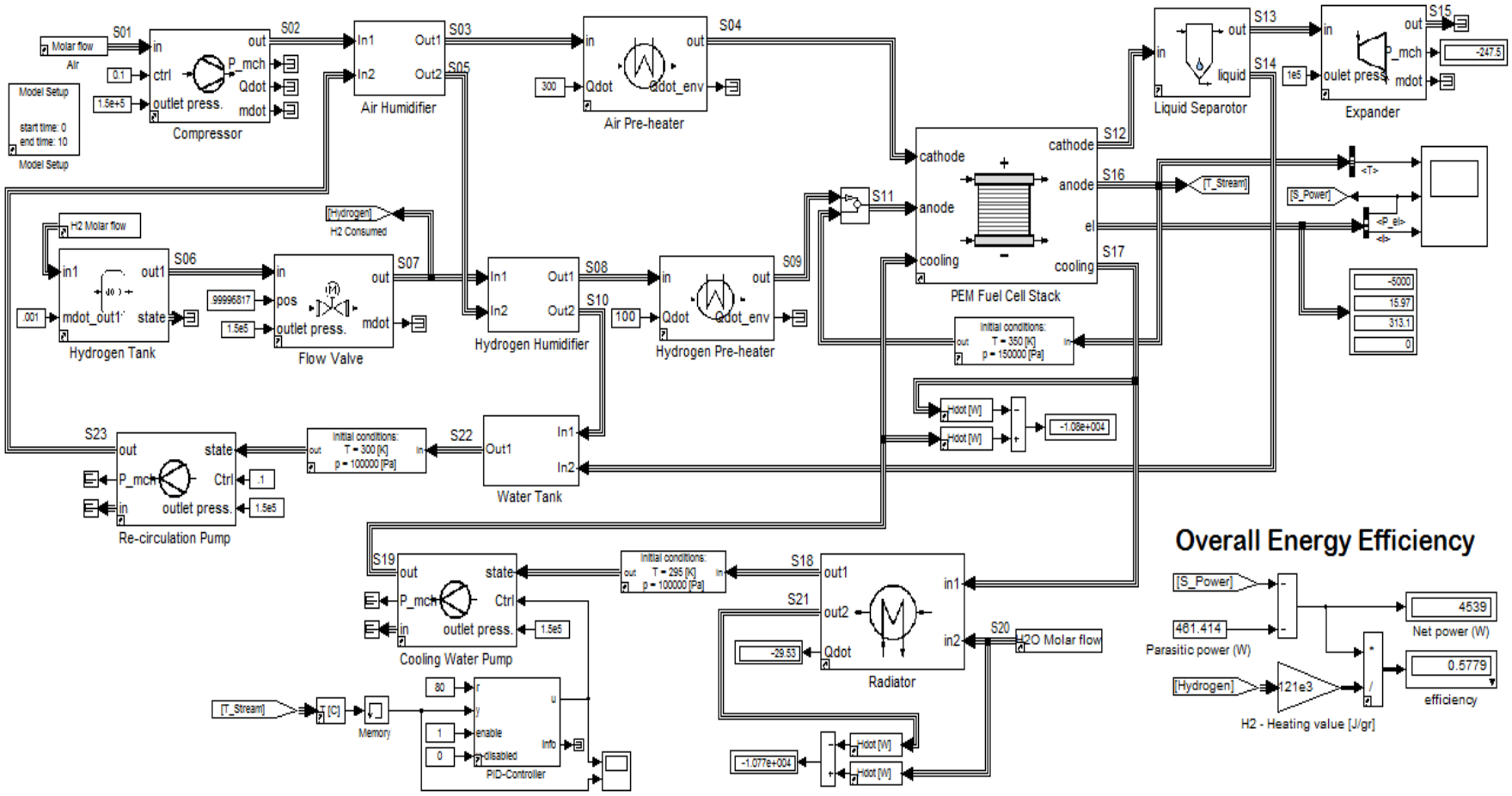


Figure A3: Thermolib model of system 3

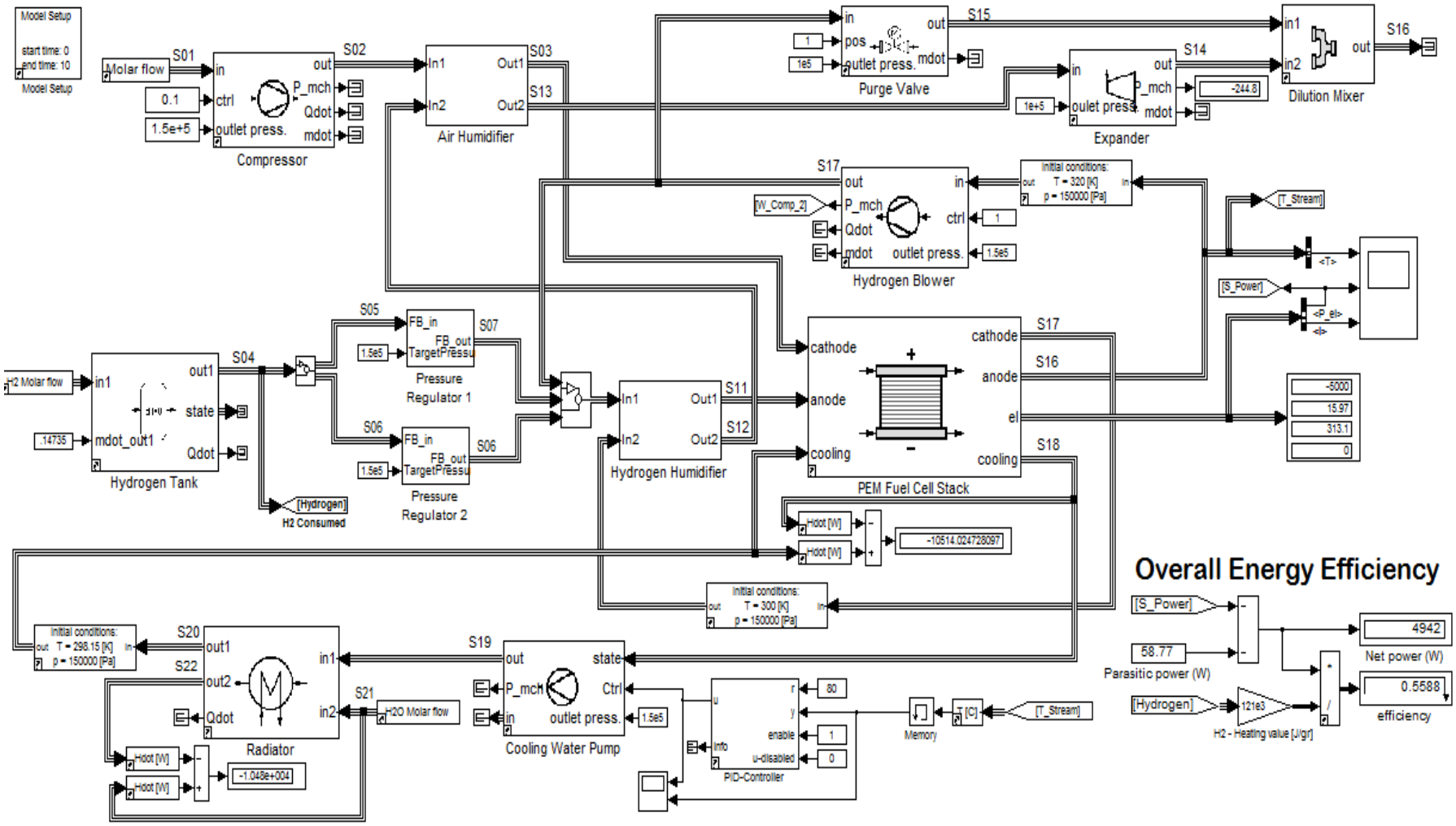


Figure A4: Thermolib model of system 4

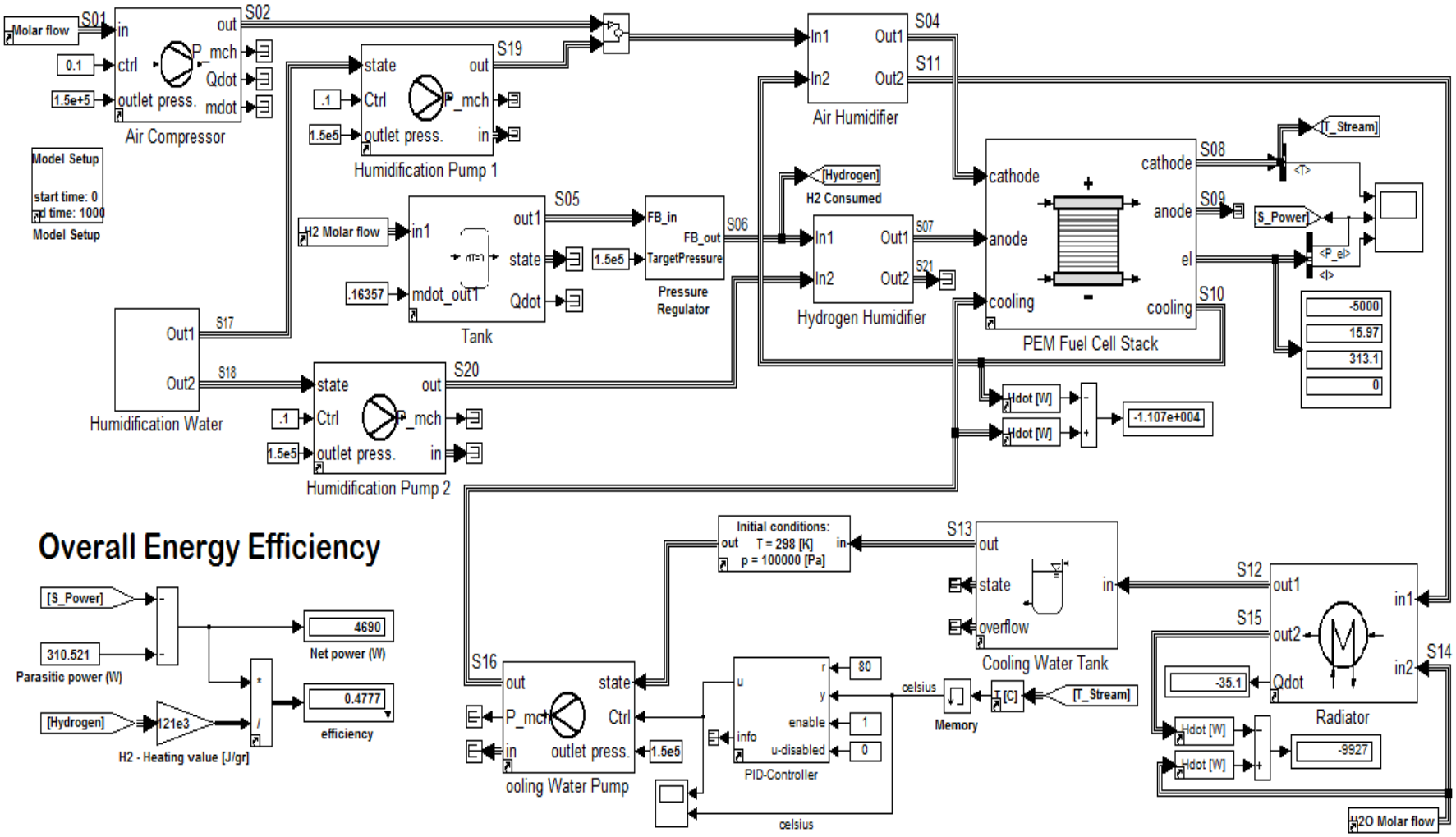


Figure A5: Thermolib model of system 5

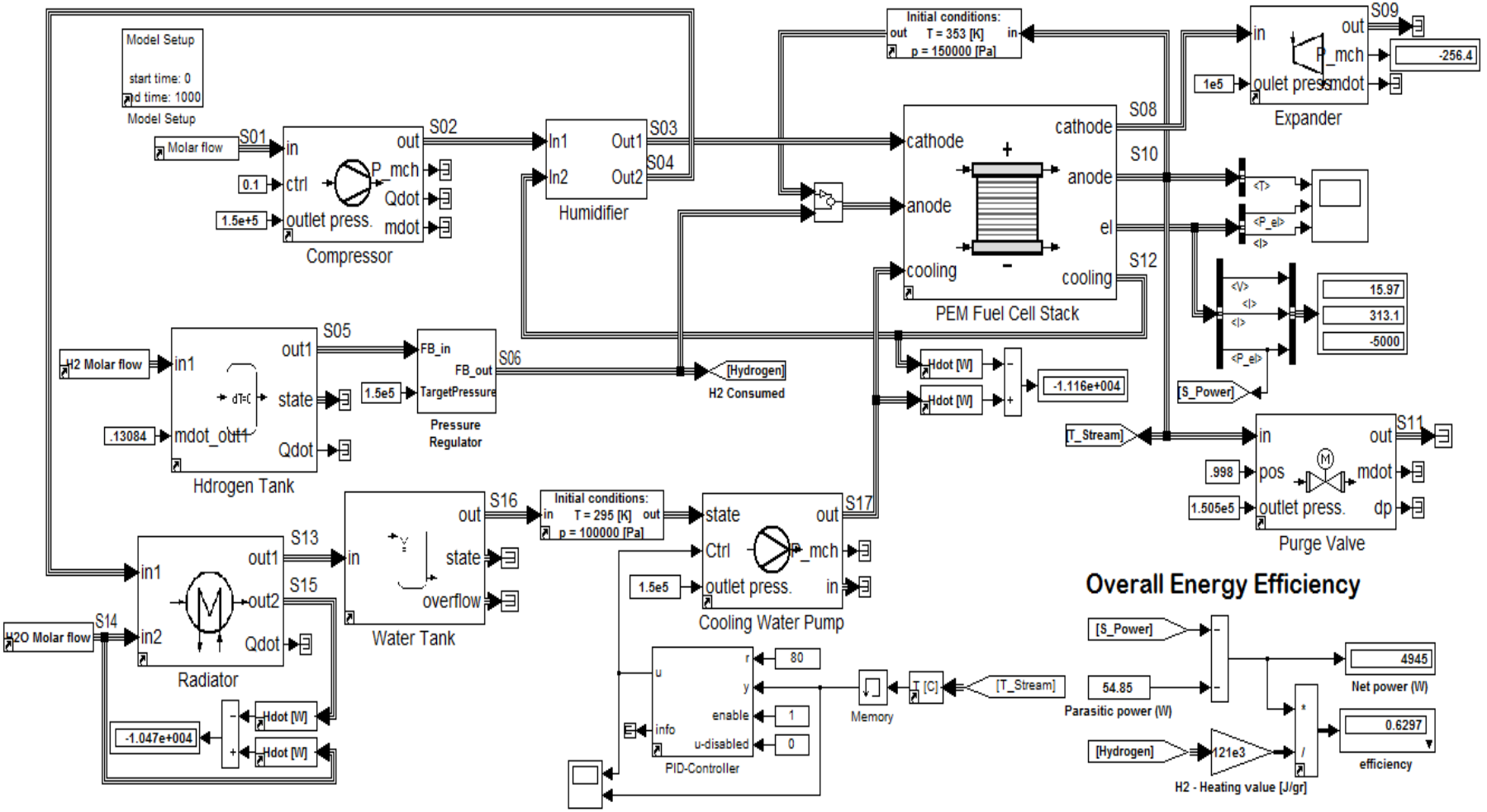


Figure A6: Thermolib model of the proposed system

Appendix B: Stream Properties Obtained by Simulation

Table B1: Stream properties of system 1

Stream	T (K)	H (W)	h_o (J/mol)	S (W/K)	s_o (J/mol.K)	Mole fraction (x)				f (mol/sec)	ψ_{ph}(J/mol)	ψ_{ch}(J/mol)	Total Exergy (W)
						H_2	O_2	H_2O	N_2				
S01	298	-968	-4620	42	199	-	0.2060	0.0191	0.7749	0.2095	0.00	115.35	24.16
S02	335	-744	-4620	42	199	-	0.2060	0.0191	0.7749	0.2095	1065.42	115.35	247.34
S03	336	-8429	-41347	49	184	-	0.1787	0.1490	0.6723	0.2414	1361.73	810.32	524.43
S04	336	-1015690	-285731	284	70	-	-	1	-	3.5893	131.61	3120.00	11670.84
S05	300	3	4	6	131	1	-	-	-	0.0649	11961.61	238500.00	16255.16
S06	300	3	4	8	131	1	-	-	-	0.0649	1005.67	238500.00	15544.11
S07	311	29	4	10	131	1	-	-	-	0.0811	1012.86	238500.00	19430.72
S08	311	-1015000	4	0	131	1	-	-	-	0.0000	38966.93	238500.00	0.00
S09	302	-1030440	-285731	258	70	-	-	1	-	3.6110	4.46	3120.00	11282.53
S10	302	-1033640	-285731	258	70	-	-	1	-	3.6212	6.54	3120.00	11321.88
S11	298	-1034690	-285731	254	70	-	-	1	-	3.6212	4.67	3120.00	11315.11
S12	298	-1142920	-285731	281	70	-	-	1	-	4.0000	7.60	3120.00	12510.42
S13	302	-1141890	-285731	284	70	-	-	1	-	4.0000	6.53	3120.00	12506.13
S14	353	-24946	-104324	52	152	-	0.0391	0.3683	0.5927	0.2739	1796.70	2899.77	1286.33
S15	353	26	4	2	131	1	-	-	-	0.0162	1137.33	238500.00	3888.16
S16	353	26	4	2	131	1	-	-	-	0.0162	1137.33	238500.00	3888.16
S17	341	-1023270	-285731	290	70	-	-	1	-	3.6212	204.73	3120.00	12039.57
S18	353	-18710	-88649	50	159	-	0.0424	0.3137	0.6439	0.2521	2320.13	2368.70	1182.10
S19	353	-6136	-285731	2	70	-	-	1	-	0.0218	331.48	3120.00	75.19
S20	353	-18710	-88649	51	159	-	0.0424	0.3137	0.6439	0.2521	1319.16	2368.63	929.72
S21	300	0	-285731	0	70	1	-	-	-	0.0000	306670.34	3120.00	0.00

Table B2: Stream properties of system 2

Stream	T (K)	H (W)	h_o (J/mol)	S (W/K)	s_o (J/mol.K)	Mole fraction (x)				f (mol/sec)	ψ_{ph}(J/mol)	ψ_{ch}(J/mol)	Total Exergy (W)
						H2	O2	H2O	N2				
S01	298	-968	-4620	42	199	-	0.2060	0.0191	0.7749	0.2095	0.00	115.35	24.16
S02	335	-744	-4620	42	199	-	0.2060	0.0191	0.7749	0.2095	1065.43	115.35	247.34
S03	315	-2691	-13745	43	197	-	0.1989	0.0528	0.7483	0.2169	910.39	227.83	246.93
S04	315	-37373	-285731	10	70	-	-	1	-	0.1313	2.70	3120.00	410.02
S05	300	4	4	10	131	1	-		-	0.0747	1005.66	238500.00	17879.77
S06	298	-40	-602	10	131	0.9975	-	0.0025	-	0.0813	1103.63	237888.74	19439.71
S07	313	-987	-12816	11	133	0.9504	-	0.0496	-	0.0854	1025.93	226751.76	19446.54
S08	313	-38352	-285731	10	70	-	-	1	-	0.1347	27.09	3120.00	424.03
S09	353	-18060	-86509	50	160	-	0.0429	0.3062	0.6509	0.2494	2272.26	2298.86	1140.01
S10	298	-11411	-53041	36	175	-	0.0501	0.1897	0.7602	0.2135	836.37	1270.24	449.81
S11	298	-10249	-285731	3	70	-	-	1	-	0.0359	2.59	3120.00	112.01
S12	298	-285731	-285731	70	70	-	-	1	-	1.0000	5.28	3120.00	3125.28
S13	346	-282182	-285731	81	70	-	-	1	-	1.0000	256.26	3120.00	3376.26
S14	353	-992	-58032	3	122	0.7929	-	0.2071	-	0.0205	1699.32	190268.29	3928.75
S15	298	-128	-7363	2	134	0.9695	-	0.0305	-	0.0167	1120.49	231256.14	3889.29
S16	298	-1065	-285731	0	70	-	-	1	-	0.0037	26.79	3120.00	11.73
S17	298	-285731	-285731	70	70	-	-	1	-	1.0000	5.28	3120.00	3125.28
S18	300	-285625	-285731	71	70	-	-	1	-	1.0000	5.55	3120.00	3125.55
S19	300	-11310	-285731	3	70	-	-	1	-	0.0396	3.98	3120.00	123.71
S20	298	-130	-7363	2	134	0.9695	-	0.0305	-	0.0167	1000.99	231256.14	3887.29
S21	298	-52	-7363	1	134	0.9695	-	0.0305	-	0.0067	1001.02	231256.14	1553.23
S22	289	0	-7363	0	134	0.9695	-	0.0305	-	0.0000	47197.77	231256.14	0.00
S23	340	-961406	-285731	271	70	-	-	1	-	3.4011	279.64	3120.00	11562.52
S24	339	-961566	-285731	271	70	-	-	1	-	3.4011	186.31	3120.00	11245.10
S25	334	-11201	-285731	3	70	-	-	1	-	0.0396	418.03	3120.00	140.10
S26	298	-971798	-285731	239	70	-	-	1	-	3.4011	3.77	3120.00	10624.26
S27	298	-1428660	-285731	351	70	-	-	1	-	5.0000	5.59	3120.00	15627.95
S28	326	-1418460	-285731	384	70	-	-	1	-	5.0000	90.80	3120.00	16053.99
S29	298	-971799	-285731	239	70	-	-	1	-	3.4011	3.48	3120.00	10623.26
S30	334	-78579	-285731	22	70	-	-	1	-	0.2775	147.49	3120.00	906.86
S31	334	-39291	-285731	11	70	-	-	1	-	0.1388	140.28	3120.00	452.43
S32	334	-39291	-285731	11	70	-	-	1	-	0.1388	140.28	3120.00	452.43

Table B3: Stream properties of system 3

Stream	T (K)	H (W)	h_o (J/mol)	S (W/K)	s_o (J/mol.K)	Mole fraction (x)				f (mol/sec)	ψ_{ph}(J/mol)	ψ_{ch}(J/mol)	Total Exergy (W)
						H2	O2	H2O	N2				
S01	298	-968	-4620	42	199	-	0.2060	0.0191	0.7749	0.2095	0.00	115.35	24.16
S02	335	-744	-4620	42	199	-	0.2060	0.0191	0.7749	0.2095	1065.43	115.35	247.34
S03	304	-1507	-7286	42	200	-	0.2037	0.0301	0.7662	0.2119	1005.83	142.18	243.21
S04	352	-1207	-7286	43	200	-	0.2037	0.0301	0.7662	0.2119	1133.63	142.18	270.28
S05	352	-78505	-285731	20	70	-	-	1	-	0.2752	0.04	3120.00	858.52
S06	300	0	4	0	131	1	-	-	-	0.0005	11961.64	238500.00	124.24
S07	300	3	4	8	131	1	-	-	-	0.0649	1005.64	238500.00	15546.65
S08	301	-386	-5871	9	133	0.9757	-	0.0243	-	0.0663	823.70	232709.84	15473.19
S09	352	-286	-5871	9	133	0.9757	-	0.0243	-	0.0663	951.19	232709.84	15481.63
S10	301	-78114	-285731	19	70	-	-	1	-	0.2735	4.16	3120.00	854.61
S11	330	-2597	-32896	13	128	0.8804	-	0.1196	-	0.0922	1212.22	210476.23	19508.85
S12	353	-16838	-82361	49	162	-	0.0438	0.2918	0.6644	0.2443	2424.67	2165.23	1121.34
S13	353	-16838	-82361	49	162	-	0.0438	0.2918	0.6644	0.2443	2180.59	2165.23	1061.71
S14	353	0	-285731	0	70	-	-	1	-	0.0000	0.00	3120.00	0.00
S15	341	-17086	-82361	49	162	-	0.0438	0.2918	0.6644	0.2443	924.54	2165.23	754.85
S16	353	-2769	-114697	4	109	0.5956	-	0.4044	-	0.0272	2057.45	145110.11	4009.86
S17	339	-1035410	-285731	291	70	-	-	1	-	3.6615	179.12	3120.00	12079.83
S18	298	-1046210	-285731	257	70	-	-	1	-	3.6615	4.02	3120.00	11438.69
S19	298	-1046210	-285731	257	70	-	-	1	-	3.6615	4.02	3120.00	11438.69
S20	298	-2285850	-285731	562	70	-	-	1	-	8.0000	6.35	3120.00	25010.83
S21	317	-2275080	-285731	597	70	-	-	1	-	8.0000	43.43	3120.00	25307.42
S22	300	-78125	-285731	19	70	-	-	1	-	0.2735	4.01	3120.00	854.57
S23	300	-79266	-285731	20	70	-	-	1	-	0.2775	3.13	3120.00	866.80

Table B4: Stream properties of system 4

Stream	T (K)	H (W)	h_o (J/mol)	S (W/K)	s_o (J/mol.K)	Mole fraction (x)				f (mol/sec)	ψ_{ph}(J/mol)	ψ_{ch}(J/mol)	Total Exergy (W)
						H2	O2	H2O	N2				
S01	298	-968	-4620	42	199	-	0.2060	0.0191	0.7749	0.2095	0.00	115.35	24.16
S02	335	-744	-4620	42	199	-	0.2060	0.0191	0.7749	0.2095	1065.43	115.35	247.34
S03	335	-744	-4620	42	199	-	0.2060	0.0191	0.7749	0.2095	1065.43	115.35	247.34
S04	300	5	4	6	131	1	-	-	-	0.0731	13198.92	238500.00	18396.75
S05	300	3	4	5	131	1	-	-	-	0.0512	11961.61	238500.00	12814.42
S06	300	1	4	2	131	1	-	-	-	0.0219	11961.65	238500.00	5491.90
S07	300	3	4	7	131	1	-	-	-	0.0512	1005.48	238500.00	12253.82
S08	300	1	4	3	131	1	-	-	-	0.0219	1005.73	238500.00	5251.67
S09	300	4	4	9	131	1	-	-	-	0.0731	3453.18	238500.00	17684.43
S10	305	17	4	9	131	1	-	-	-	0.0811	7805.72	238500.00	19985.02
S11	305	17	4	10	131	1	-	-	-	0.0811	1007.80	238500.00	19433.45
S12	353	-16167	-80361	48	163	-	0.0442	0.2848	0.6710	0.2419	2551.20	2101.68	1125.66
S13	353	-16267	-80361	48	163	-	0.0442	0.2848	0.6710	0.2419	2137.85	2101.68	1025.66
S14	340	-16512	-80361	48	163	-	0.0442	0.2848	0.6710	0.2419	881.30	2101.68	721.67
S15	300	0	4	0	131	1	-	-	-	0.0000	38966.93	238500.00	0.00
S16	340	-16512	-80361	49	163	-	0.0442	0.2848	0.6710	0.2419	758.07	2101.68	691.85
S17	353	-16267	-80361	48	163	-	0.0442	0.2848	0.6710	0.2419	2137.85	2101.68	1025.66
S18	353	21	4	2	131	1	-	-	-	0.0162	829.11	238500.00	3883.78
S19	353	13	4	1	131	1	-	-	-	0.0080	1137.26	238500.00	1928.79
S20	340	-982688	-285731	277	70	-	-	1	-	3.4755	147.49	3120.00	11356.18
S21	340	-982548	-285731	277	70	-	-	1	-	3.4755	187.77	3120.00	11496.18
S22	298	-993068	-285731	244	70	-	-	1	-	3.4755	1.25	3120.00	10847.93
S23	298	-2285850	-285731	562	70	-	-	1	-	8.0000	6.35	3120.00	25010.83
S24	316	-2275360	-285731	596	70	-	-	1	-	8.0000	42.68	3120.00	25301.42

Table B5: Stream properties of system 5

Stream	T (K)	H (W)	h_o (J/mol)	S (W/K)	s_o (J/mol.K)	Mole fraction (x)				f (mol/sec)	ψ_{ph}(J/mol)	ψ_{ch}(J/mol)	Total Exergy (W)
						H2	O2	H2O	N2				
S01	298	-968	-4620	42	199	-	0.2060	0.0191	0.7749	0.2095	0.00	115.35	24.16
S02	335	-744	-4620	42	199	-	0.2060	0.0191	0.7749	0.2095	1065.43	115.35	247.34
S03	305	-32464	-101623	50	156	-	0.1346	0.3589	0.5065	0.3205	669.27	2666.56	1069.09
S04	332	-6890	-34270	47	187	-	0.1839	0.1243	0.6918	0.2346	956.38	637.59	374.02
S05	300	4	4	7	131	1	-	-	-	0.0811	11961.59	238500.00	20321.43
S06	300	4	4	10	131	1	-	-	-	0.0811	1005.63	238500.00	19432.50
S07	293	-311	-3740	11	132	0.9845	-	0.0155	-	0.0824	1128.35	234792.22	19442.52
S08	353	-22934	-99716	52	154	-	0.0400	0.3522	0.6077	0.2671	2208.14	2740.29	1321.73
S09	353	-280	-19486	2	131	0.9271	-	0.0729	-	0.0175	1185.96	220700.89	3883.60
S10	337	-1168990	-285731	327	70	-	-	1	-	4.1319	164.67	3120.00	13572.01
S11	332	-1194640	-285731	330	70	-	-	1	-	4.2178	129.33	3120.00	13704.93
S12	300	-1204600	-285731	298	70	-	-	1	-	4.2178	3.72	3120.00	13175.12
S13	300	-1204589	-285731	298	70	-	-	1	-	4.2178	2.37	3120.00	13169.42
S14	298	-1142920	-285731	281	70	-	-	1	-	4.0000	7.60	3120.00	12510.42
S15	332	-1133000	-285731	313	70	-	-	1	-	4.0000	93.38	3120.00	12853.54
S16	300	-1180070	-285731	292	70	-	-	1	-	4.1319	3.14	3120.00	12904.60
S17	298	-158605	-285731	39	70	-	-	1	-	0.5551	0.01	3120.00	1731.87
S18	298	-158605	-285731	39	70	-	-	1	-	0.5551	0.01	3120.00	1731.87
S19	298	-31721	-285731	8	70	-	-	1	-	0.1110	3.07	3120.00	346.71
S20	298	-31721	-285731	8	70	-	-	1	-	0.1110	3.07	3120.00	346.71
S21	293	-31396	-285731	8	70	-	-	1	-	0.1097	6.36	3120.00	343.09

Table B6: Stream properties of proposed system configuration

Stream	T (K)	H (W)	h_o (J/mol)	S (W/K)	s_o (J/mol.K)	Mole fraction (x)				f (mol/sec)	ψ_{ph}(J/mol)	ψ_{ch}(J/mol)	Total Exergy (W)
						H2	O2	H2O	N2				
S01	298	-968	-4620	42	199	-	0.2060	0.0191	0.7749	0.2095	0.00	115.35	24.1628
S02	335	-744	-4620	42	199	-	0.2060	0.0191	0.7749	0.2095	1065.42	115.35	247.3393
S03	333	-7021	-35178	47	187	-	0.1832	0.1275	0.6893	0.2355	1267.60	659.01	453.7115
S04	333	-1180500	-285731	326	70	-	-	1	-	4.1685	134.68	3120.00	13566.9615
S05	300	3	4	6	131	1	-	-	-	0.0649	11961.38	238500.00	16255.1439
S06	300	3	4	8	131	1	-	-	-	0.0649	1005.67	238500.00	15544.1098
S07	311	29	4	10	131	1	-	-	-	0.0811	1012.86	238500.00	19430.7201
S08	353	-23172	-100299	52	154	-	0.0399	0.3542	0.6058	0.2679	2202.71	2760.28	1329.8239
S09	343	-23441	-100299	52	154	-	0.0399	0.3542	0.6058	0.2679	1080.27	2760.28	1029.0691
S10	353	26	4	2	131	1	-	-	-	0.0162	1137.33	238500.00	3888.1636
S11	300	0	4	0	131	1	-	-	-	0.0000	38966.93	238500.00	0.0000
S12	336	-1186680	-285731	332	70	-	-	1	-	4.1945	185.00	3120.00	13862.7408
S13	300	-1190620	-285731	294	70	-	-	1	-	4.1685	2.81	3120.00	13017.2783
S14	298	-1142920	-285731	281	70	-	-	1	-	4.0000	7.60	3120.00	12510.4161
S15	333	-1132850	-285731	313	70	-	-	1	-	4.0000	104.42	3120.00	12897.6967
S16	300	-1190500	-285731	295	70	-	-	1	-	4.1685	4.35	3120.00	13023.6832
S17	300	-1197930	-285731	296	70	-	-	1	-	4.1945	4.62	3120.00	13106.1301

Appendix C: Cost Estimates and Economic Parameters

Table C1: Systems and equipment costs estimates

	System 1		System 2		System 3		System 4		System 5		Proposed System	
Components	**Units**	**Cost ($)**	**Units**	**Cost ($)**	**Units**	**Cost ($)**	**Units**	**Cost ($)**	**Units**	**Cost ($)**	**Units**	**Cost ($)**
Stack	1	1818.34	1	1818.34	1	1818.34	1	1818.34	1	1818.34	1	1818.34
Compressor	1	160.63	1	160.63	-	-	-	-	1	160.63	-	-
Compressor Expander Module (CEM)	-	-	-	-	1	431.56	1	431.56	-	-	1	431.56
Hydrogen Blower	1	293.37	1	293.27	-	-	1	292.37	-	-	-	-
Membrane Humidifier (for air)	1	146.38	1	146.38	1	146.38	1	146.38	1	146.38	1	146.38
Membrane Humidifier (for hydrogen)	-	-	1	77.81	1	77.81	-	-	1	77.81	-	-
Enthalpy Wheel Humidifier	-	-	-	-	-	-	1	87.62	-	-	-	-
Hydrogen Ejector	-	-	-	-	-	-	1	56.18	-	-	-	-
Hydrogen Demister	-	-	-	-	-	-	1	80.44	-	-	-	-
Air Demister	-	-	-	-	-	-	1	205.73	-	-	-	-
Mixer	-	-	-	-	-	-	1	35.61	-	-	-	-
Purge Valve	1	19.78	1	19.78	-	-	2	39.56	-	-	1	19.78
Check Valve	-	-	-	-	-	-	2	26.38	-	-	-	-
Air Filter	-	-	1	5.28	-	-	1	5.28	-	-	-	-
Air Cooler	-	-	1	56.71	-	-	-	-	-	-	-	-
Radiator	1	85.30	1	85.30	1	85.30	1	85.30	1	85.30	1	85.30
Radiator Fan	1	98.91	1	98.91	1	98.91	1	98.91	1	98.91	1	98.91
Re-circulation Pump	-	-	1	39.65	1	39.65	-	-	2	79.30	-	-
Cooling Pump	1	83.08	1	83.08	1	83	1	83.08	1	83.08	1	83.08
Proportionate Valve	2	81.64	1	40.82	1	40.82	2	81.64	1	40.82	2	40.82
Condenser	-	-	2	513.90	-	-	-	-	-	-	-	-
Control, Wiring, Piping		367.00		367.00		367.00		367.00		367.00		367.00
Design Engineering and Contingencies		1261.77		1522.74		1275.54		1576.55		1183.03		1236.47
System Cost ($)		**4416.20**		**5329.60**		**4464.39**		**5517.93**		**4140.60**		**4327.64**

Table C2: Economic analysis results

Systems	System 1	System 2	System 3	System 4	System 5	Proposed Syst.
Estimated Cost ($)	4416.20	5329.60	4464.39	5517.93	4140.60	4327.64
Net power (kW)	4.671	4.654	4.539	4.941	4.689	4.945
Cost per kW of Net Power ($/kW)	945.42	1145.17	983.65	1116.71	882.96	875.13
Fuel Consumption (Kg/h)	0.471	0.542	0.471	0.530	0.589	0.471
Fixed Capital Investment ($)	3709.61	4476.86	3750.09	4635.06	3478.10	3635.22
Annual Fuel Cost ($)	3967.91	4564.12	3968.55	4468.60	4960.49	3967.91
Annual Output (kWh)	30269.11	30157.92	29410.04	32019.17	30387.82	32044.57
Annual Maintenance Cost ($)	397.46	479.66	401.80	496.61	372.65	389.49
Annual Operating Cost ($)	4365.36	5043.79	4370.35	4965.21	5333.14	4357.39
Annual Income (Sales) ($)	5599.79	5579.22	5440.86	5923.55	5621.75	5928.25
Annual Operating Income ($)	1234.42	535.43	1070.51	958.34	288.60	1570.85
Annual Depreciation ($)	247.31	298.46	250.01	309.00	231.87	242.35
Income Before Tax ($)	987.11	236.97	820.50	649.33	56.73	1328.50
Income After Tax ($)	740.34	177.73	615.38	487.00	42.55	996.38
Annual Cash Income ($)	987.64	476.19	865.38	796.00	274.42	1238.73
Annual Cash Flow ($)	4697.25	4953.05	4615.47	5431.07	3752.53	4873.94
Pay Back Period (yrs)	4	9	4	6	13	3
Proceeds Per Dollar ($)	4	2	3	3	1	5
ROI (%)	20	4	16	11	1	27